U.S. Department of Transportation

Federal Railroad Administration

Measurement of Wheel Load Environment of a Standard 3-piece Truck

Office of Research,
Development and Technology
Washington, DC 20590

DOT/FRA/ORD-17-25

Final Report
December 2017

NOTICE

This document is disseminated under the sponsorship of the Department of Transportation in the interest of information exchange. The United States Government assumes no liability for its contents or use thereof. Any opinions, findings and conclusions, or recommendations expressed in this material do not necessarily reflect the views or policies of the United States Government, nor does mention of trade names, commercial products, or organizations imply endorsement by the United States Government. The United States Government assumes no liability for the content or use of the material contained in this document.

NOTICE

The United States Government does not endorse products or manufacturers. Trade or manufacturers' names appear herein solely because they are considered essential to the objective of this report.

REPORT DOCUMENTATION PAGE

Form Approved
OMB No. 0704-0188

1. AGENCY USE ONLY (Leave blank)	2. REPORT DATE	3. REPORT TYPE AND DATES COVERED
	December 2017	Technical Report- November 2010

4. TITLE AND SUBTITLE
Measurement of Wheel Load Environment of a Standard 3-piece Truck

5. FUNDING NUMBERS
DTFR-53-00-C-00012
Task Order 245

6. AUTHOR(S)
Scott Cummings, John Punwani and Richard Reiff

7. PERFORMING ORGANIZATION NAME(S) AND ADDRESS(ES)
Transportation Technology Center, Inc
55500 DOT Road
Pueblo, CO 81001

8. PERFORMING ORGANIZATION REPORT NUMBER

9. SPONSORING/MONITORING AGENCY NAME(S) AND ADDRESS(ES)
U.S. Department of Transportation
Federal Railroad Administration
Office of Research, Development and Technology
1200 New Jersey Avenue, SE
Washington, DC 20590

10. SPONSORING/MONITORING AGENCY REPORT NUMBER
DOT/FRA/ORD-17/25

11. SUPPLEMENTARY NOTES
COR: John Punwani

12a. DISTRIBUTION/AVAILABILITY STATEMENT
This document is available to the public through the FRA Web site at http://www.fra.dot.gov.

12b. DISTRIBUTION CODE

13. ABSTRACT (Maximum 200 words)
To increase the understanding of the conditions under which wheel rolling contact fatigue (RCF) damage accumulates, wheel load environment data was collected from a car running in revenue service and analyzed to assess the predicted wheel RCF damage using shakedown theory. The car used for the tests had 3-piece trucks. A track inspection team visited critical track locations to record relevant information such as rail RCF, rail profile, curve superelevation, and friction conditions. This study found that track curvature is highly influential in determining wheel and rail RCF damage. Nearly all significant predictions of RCF were recorded on curves of at least 4 degrees. Other important factors include the curve unbalance condition and wheel/rail coefficient of friction. Rail profile and track friction conditions were not found to be major factors in this analysis. Observed rail RCF condition correlated reasonably well with predictions when considering extenuating factors such as rail age and curve unbalance conditions.

14. SUBJECT TERMS
Rolling contact fatigue, RCF, wheel shelling, shakedown

15. NUMBER OF PAGES
44

16. PRICE CODE

17. SECURITY CLASSIFICATION OF REPORT	18. SECURITY CLASSIFICATION OF THIS PAGE	19. SECURITY CLASSIFICATION OF ABSTRACT	20. LIMITATION OF ABSTRACT
Unclassified	Unclassified	Unclassified	

NSN 7540-01-280-5500
Standard Form 298 (Rev. 2-89)
Prescribed by ANSI Std. 239-18
298-102

METRIC/ENGLISH CONVERSION FACTORS

ENGLISH TO METRIC	METRIC TO ENGLISH
LENGTH (APPROXIMATE)	**LENGTH (APPROXIMATE)**
1 inch (in) = 2.5 centimeters (cm)	1 millimeter (mm) = 0.04 inch (in)
1 foot (ft) = 30 centimeters (cm)	1 centimeter (cm) = 0.4 inch (in)
1 yard (yd) = 0.9 meter (m)	1 meter (m) = 3.3 feet (ft)
1 mile (mi) = 1.6 kilometers (km)	1 meter (m) = 1.1 yards (yd)
	1 kilometer (km) = 0.6 mile (mi)
AREA (APPROXIMATE)	**AREA (APPROXIMATE)**
1 square inch (sq in, in^2) = 6.5 square centimeters (cm^2)	1 square centimeter (cm^2) = 0.16 square inch (sq in, in^2)
1 square foot (sq ft, ft^2) = 0.09 square meter (m^2)	1 square meter (m^2) = 1.2 square yards (sq yd, yd^2)
1 square yard (sq yd, yd^2) = 0.8 square meter (m^2)	1 square kilometer (km^2) = 0.4 square mile (sq mi, mi^2)
1 square mile (sq mi, mi^2) = 2.6 square kilometers (km^2)	10,000 square meters (m^2) = 1 hectare (ha) = 2.5 acres
1 acre = 0.4 hectare (he) = 4,000 square meters (m^2)	
MASS - WEIGHT (APPROXIMATE)	**MASS - WEIGHT (APPROXIMATE)**
1 ounce (oz) = 28 grams (gm)	1 gram (gm) = 0.036 ounce (oz)
1 pound (lb) = 0.45 kilogram (kg)	1 kilogram (kg) = 2.2 pounds (lb)
1 short ton = 2,000 pounds (lb) = 0.9 tonne (t)	1 tonne (t) = 1,000 kilograms (kg)
	= 1.1 short tons
VOLUME (APPROXIMATE)	**VOLUME (APPROXIMATE)**
1 teaspoon (tsp) = 5 milliliters (ml)	1 milliliter (ml) = 0.03 fluid ounce (fl oz)
1 tablespoon (tbsp) = 15 milliliters (ml)	1 liter (l) = 2.1 pints (pt)
1 fluid ounce (fl oz) = 30 milliliters (ml)	1 liter (l) = 1.06 quarts (qt)
1 cup (c) = 0.24 liter (l)	1 liter (l) = 0.26 gallon (gal)
1 pint (pt) = 0.47 liter (l)	
1 quart (qt) = 0.96 liter (l)	
1 gallon (gal) = 3.8 liters (l)	
1 cubic foot (cu ft, ft^3) = 0.03 cubic meter (m^3)	1 cubic meter (m^3) = 36 cubic feet (cu ft, ft^3)
1 cubic yard (cu yd, yd^3) = 0.76 cubic meter (m^3)	1 cubic meter (m^3) = 1.3 cubic yards (cu yd, yd^3)
TEMPERATURE (EXACT)	**TEMPERATURE (EXACT)**
[(x-32)(5/9)] °F = y °C	[(9/5) y + 32] °C = x °F

QUICK INCH - CENTIMETER LENGTH CONVERSION

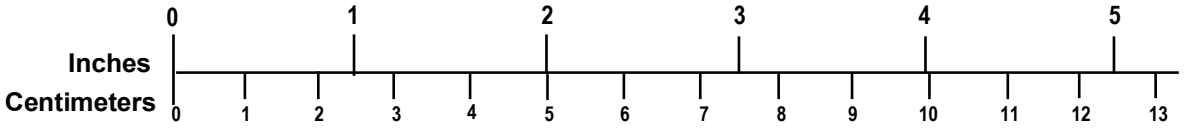

QUICK FAHRENHEIT - CELSIUS TEMPERATURE CONVERSIO

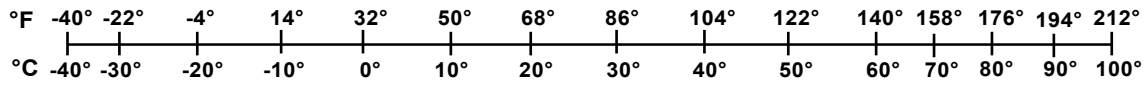

For more exact and or other conversion factors, see NIST Miscellaneous Publication 286, Units of Weights and Measures. Price $2.50 SD Catalog No. C13 10286

Updated 6/17/98

Contents

Illustrations

Tables

Executive Summary

The Federal Railroad Administration (FRA) contracted the Transportation Technology Center, Inc. (TTCI) in 2010 to evaluate root causes of wheel tread fatigue damage by collecting wheel load environment data from a car running in revenue service. The load environment of a wheelset in a revenue service coal car with standard 3-piece trucks was recorded using a load measuring wheelset. This data was analyzed to assess the predicted rolling contact fatigue (RCF) damage through the use of shakedown theory. A track inspection team was dispatched to seven critical track locations to record relevant information, such as rail RCF, rail profile, curve superelevation, and friction conditions.

This work shows that track curvature is highly influential in determining wheel and rail RCF damage. Nearly all significant RCF predicted locations were in curves of at least 4 degrees. The curve unbalance condition, which is a combination of curvature, track superelevation, and train speed, is also an important factor in RCF. Wheel/rail coefficient of friction in curves can be a factor in RCF. Rail profile and track condition at the locations investigated were not found to be major factors in this analysis. Observed rail RCF condition correlated reasonably well with predictions when considering extenuating factors such as rail age and curve unbalance conditions.

Recommendations for reducing wheel and rail RCF damage include controlling the wheel/rail coefficient of friction where track curvature is 4 degrees or tighter and reducing the superelevation in specific curves where the typical train speed is much slower than the design speed of the curve.

Data from two loaded trips of a coal car operating on a route over 1,000 miles was recorded and analyzed. Based on this data, RCF damage was predicted to occur at 157 unique track locations for a total distance of less than 2 miles. Most of these sites are located in 4 to 7 degree curves. In general, wheel/rail forces had good repeatability at individual curves when comparing the first and second trips.

Six out of seven of the track inspection sites were located in 4-degree curves; three where RCF was predicted and three comparison curves where RCF was not predicted. Moderate to severe RCF damage was found on the rails at the three 4-degree curve sites with predicted RCF, including one site with 1½-year-old rail. The rails were very dry at these sites, and the train was operated far below the curve balance speed. Minimal RCF damage was found at one site where RCF was not predicted. This was the only inspected site with any visible lubricant. Moderate to severe RCF damage was found at the other two sites where RCF was not predicted; however, the train speed was near the curve balance speed, and at one of these sites, the rail was significantly older than the other rails inspected.

1. Introduction

The purpose of this study was to provide information needed to better understand the effects of track and operating conditions on wheel and rail rolling contact fatigue (RCF) damage. TTCI evaluated root causes of wheel tread fatigue by collecting wheel load environment data from a car in revenue service, and then analyzing this data to assess the predicted RCF damage in a revenue service coal car. A track inspection team was dispatched to several critical sites to record relevant information, such as rail RCF, rail profile, curve superelevation, and friction conditions.

1.1 Background

Wheel tread damage is the primary cause of wheelset replacement in North America [1]. Tread damage is commonly manifested as high-impact wheels identified through the use of wheel impact load detector (WILD) systems. Voids in the wheel tread surface result in radial runout, which in turn can produce impact loads each time the portion of the wheel with the radial deviation contacts the rail. Large impact loads increase the probability of a wheel developing a shattered rim failure.

The lateral traction forces generated at the low-rail wheel of the leading wheelset of a car negotiating a curve create the conditions necessary for RCF [2]. These lateral traction forces are a result of a high angle of attack (AOA), which is a function of many parameters including truck warp, wheel/rail profiles, wheel/rail friction, and excess track superelevation.

Shelling is a fatigue based process and one mechanism by which large voids can be left in the running surface of a wheel. Many cycles of high stress create surface cracks in the wheel tread through the process of RCF. Frequently, bands of these cracks will form on the wheel tread surface. Figure 1 shows a wheel with a band of RCF cracks. As the cracks propagate and grow, they can connect and dislodge a patch of wheel tread, leaving a void in the process.

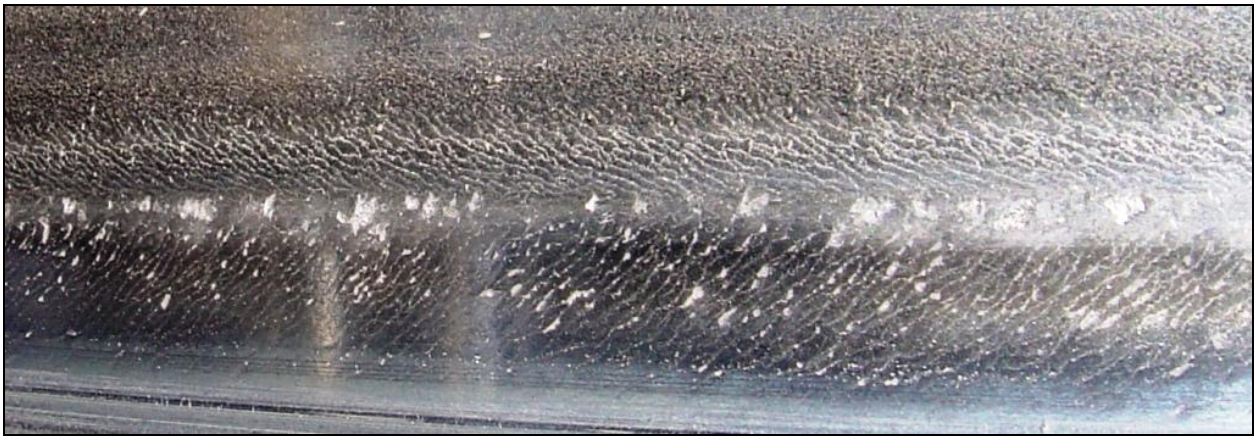

Figure 1. Wheel Tread Surface with RCF Cracks

The magnitude of the contact forces between the wheel and rail determine the fatigue damage incurred from each contact cycle. Thus, measuring the load environment of a wheel in revenue service allows for investigation of the conditions present when RCF damage occurs.

1.2 Objective

The objective of this work is to increase the understanding of the conditions under which wheel RCF damage accumulates.

1.3 Overall Approach

The load environment of a wheelset in a revenue service coal car with standard 3-piece trucks was recorded using a load measuring wheelset. The car was equipped with an unmanned data collection system. The system automatically transmitted summary data for the purpose of identifying specific track locations where RCF was predicted to occur. Based on the proximity of the identified track locations, a detailed track inspection was arranged at seven of these sites. A track inspection team was dispatched to these sites to record relevant information, such as rail RCF, rail profile, curve superelevation, and friction conditions.

1.4 Scope

Prior to the award of this FRA task order, TTCI had already begun this study under the direction of and with funding from the Wheel Defect Prevention Research Consortium. The revenue service car had already been equipped with instrumentation, a data collection system, and two generator roller bearings (including one owned by FRA) to power a bank of batteries. The scope of work for the task order that funded this project included two revenue service data collection trips, one track inspection trip, removal of the test equipment from the car, analysis of the data, and writing of the report.

1.5 Organization of the Report

This report is organized into sections describing the procedures used, analysis of wheel/rail force data, track inspection results, and the conclusion.

2. Procedure

This section of the report describes the instrumentation used to record the data and the methodology for predicting RCF damage.

2.1 Test Vehicle

An aluminum body rotary dump coal gondola was used as the test vehicle. The car had a stenciled light weight of 43,900 pounds and a stenciled load limit of 242,100 pounds. The car was equipped with standard 3-piece trucks, constant contact side bearings, and truck mounted brakes. The brakes were disabled on the A-end of the car to eliminate heat input into the instrumented wheelset installed in this truck. An FRA waiver was obtained to run the car in revenue service for a limited number of trips on specific routes with a partially disabled brake system.

2.2 Instrumentation

The instrumentation installed on the railcar included an instrumented (load measuring) wheelset (IWS) and a Global Positioning System (GPS) receiver.

2.2.1 Instrumented Wheelset

For nearly 20 years, TTCI has designed and constructed high accuracy load measuring wheelsets for measurement of wheel/rail interaction values including:

- Vertical loads
- Lateral loads
- Longitudinal loads
- Lateral position of the contact patch relative to the wheel taping line

An IWS was installed in the test vehicle in position 4, nearest to the A-end of the car. The vehicle was always oriented with the A-end of the car leading, so that the IWS was in the leading position of the leading truck. This is where the largest curving forces are expected.

Wheel/rail force at the contact patch can be divided into several components. When the plane of contact is approximately parallel to the ground, the normal force can be approximated as the vertical force, and the tangential force can be approximated as the vector sum of the lateral and longitudinal forces. In a situation where the wheel is flanging, these approximations are not accurate, because the plane of contact is not parallel to the ground. Also, complicating matters in a flanging situation is the possibility of more than one contact point between the wheel and rail.

From the available IWS measurements, the tangential force was calculated whenever the lateral contact position was no more than one-half inch inboard from the tapeline, effectively excluding any less accurate tangential force calculations, because of wheel flange contact with the rail. Figure 2 shows the contact positions considered in the analysis. The exclusion of tangential forces near the flange should be an acceptable simplification, since RCF damage on wheels is most intense outboard of the tapeline [3]. This simplification also means that all shakedown

exceedances in curves described in this report are related to the low-rail wheel, because the contact patch of the high rail wheel is located in the flange root where tangential forces are not calculated.

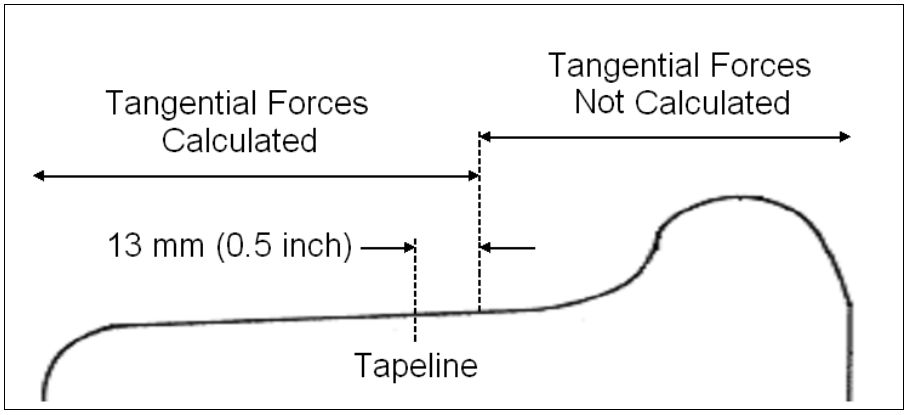

Figure 2. Wheel Profile Showing Contact Zone Considered in the Analysis

2.2.2 GPS Receiver

A GPS receiver was used to collect the following information about the test vehicle:

- Latitude
- Longitude
- Speed
- Heading

The latitude and longitude readings allowed the data to be matched up with track charts provided by the railroad. Street maps and satellite photos of the latitude and longitude of important track locations were used to identify nearby towns, road crossings, bridges, and curves. This allowed for positive identification of the mileposts associated with important track locations. The heading data from the GPS receiver allowed for an estimate of the track curvature at all locations. The curvature estimates from important track locations were compared to the curvature data listed on the track charts and found to be accurate within one half of one degree.

2.2.3 Data Collection System

TTCI has developed ruggedized unmanned data acquisition (UDAC) systems that have repeatedly proven reliable for collecting data in the vibration environment of freight railroading. The UDAC system used for this test consists of a low power usage computer and low power usage signal conditioning. Two generator bearings were installed on the wheelset in position 3 (same truck as the IWS) to charge a bank of batteries. One of the generator bearings belonged to the FRA and the other generator bearing belonged to TTCI. To minimize power usage while the car was not moving, the UDAC system shut down whenever the car sat stationary for more than 15 minutes; it rebooted whenever the car resumed travel. The UDAC was equipped with a means to transmit basic information back to TTCI via cellular telephone signal. Data from the IWS was collected at 128 samples per second and low-pass filtered at 15 Hz.

2.3 Prediction of Rolling Contact Fatigue

Shakedown theory can be used to estimate how repeated rolling contact will affect a material. Stresses produced by rolling contact might produce purely elastic strains, subsurface plastic strain, or surface plastic strain. Initial rolling contacts might produce plastic strains that result in residual stresses. These residual stresses may form such that further rolling contacts produce stresses that when combined with the residual stresses no longer exceed the elastic limit. This process is called shakedown. Contact conditions can exist such that the residual stresses will not prevent plastic deformation with repeated contact. Plastic deformation leads to fatigue damage.

Figure 3 shows the shakedown diagram. The contact stress for the rolling contact (Po) is divided by the material's shear yield stress (K) and plotted against the traction coefficient (ratio of tangential force (T) and normal force (N)). Traction coefficient values can range from zero to the wheel/rail coefficient of friction. The shakedown limit is the limit for continuous deformation under repeated loading. This limit is calculated to be slightly different, depending upon assumptions made regarding the contact conditions. The shakedown limits under full-slip conditions for pure lateral and pure longitudinal loading are plotted on the axes [4]. The exact location of the shakedown limit line is a subject of some debate. In fact, it may be more accurate to identify it as a shakedown limit zone, rather than a line. The area below this zone represents conditions where only elastic deformation is likely to take place. The area above this zone represents conditions where plastic deformation is likely to take place. Regions where the plastic deformation occurs below the surface or on the surface are labeled. Contact conditions far beyond shakedown may result in wear instead of RCF damage.

To show the IWS data on a shakedown plot, distance contours have been used. The x-axis (T/N) and y-axis (Po/K) were each broken into discrete bins, and the total distance traveled at the conditions corresponding to each bin was summed. Matlab® contour plotting functions were then used to produce contour plots with a superimposed shakedown limit. Each shakedown plot with IWS data shown in this report represents data from a specific track location such as a curve. The contours represent 2-percent increments of the total distance traveled at that location. The Matlab® contour plotting functions provide smooth contour lines based on the percent of the data in each bin.

All shakedown plots have been calculated assuming Hertzian contact between a 36-inch diameter wheel with a nonhollow transverse profile in the contact region and a rail with 14-inch crown radius. The shear yield stress was assumed to be 65,000 pounds per square inch, based on a yield stress of 113,000 pounds per square inch for AAR Class C wheel material at room temperature. Thus, the shakedown plots predicted RCF damage to the wheels. The shear yield stress of rail steel may be slightly different than wheel steel, and therefore, the predicted RCF damage to the rails is expected to be slightly different.

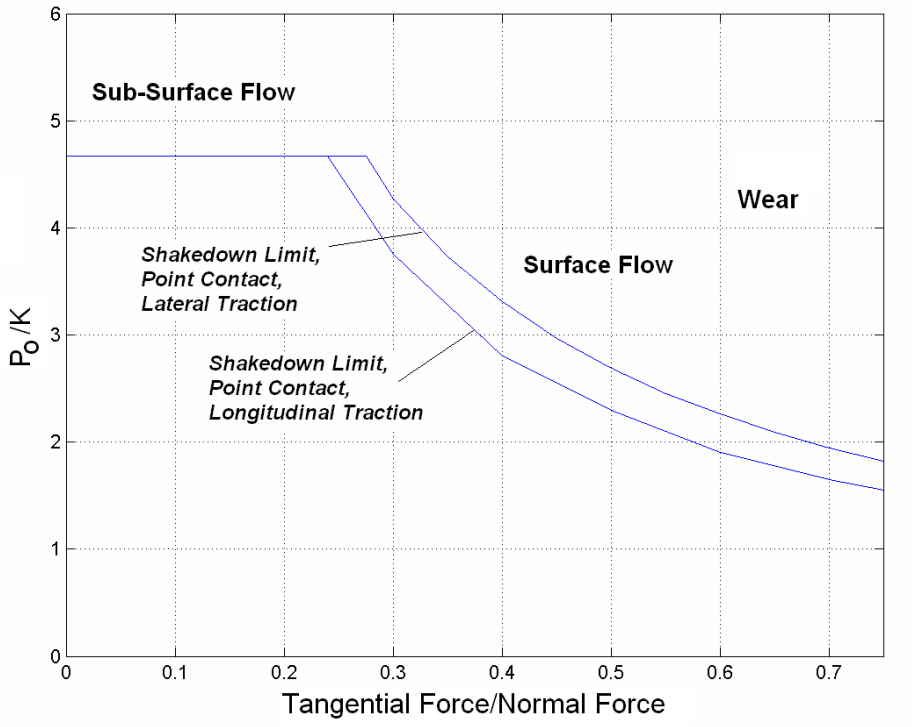

Figure 3. Shakedown Diagram

2.4 Track Inspection Procedure

Seven sites were selected for track inspection based on analysis of the IWS data. At each site, a similar inspection procedure was used. General site photographs were taken from the viewpoint at each end of the curve. The inspection crew selected two locations at each site, one approximately one third of the way through the curve and the other approximately two thirds of the way through the curve. At each of these locations, transverse rail profile measurements were recorded with a Miniprof™ profilometer. The track gage and superelevation were measured. An assessment of the lubrication status of the rail was made based on the presence or absence of lubricant or friction control material, the smoothness of the rail surface, and the presence or absence of wheel and rail metal wear flakes. General track conditions were noted. The manufacturer, manufacture year, and rail section were noted. The relative RCF damage on the rails was assessed by applying dye penetrant and taking photographs.

3. Wheel Load Environment

The load environment experienced by a wheelset in revenue service was measured with an IWS installed in the leading position of the leading truck of a revenue service coal gondola. Data was analyzed from the two trips from the mine to the power plant.

3.1 First Trip

The first loaded trip began September 2, 2010, at the mine and concluded September 5, 2010, at the power plant. A total of 1,084 miles of data was recorded with the car in the loaded condition between the mine to the power plant. Figures 4 through 6 contain histograms of the vertical, lateral, and longitudinal wheel/rail forces, respectively. Figure 7 contains a histogram of the train speed.

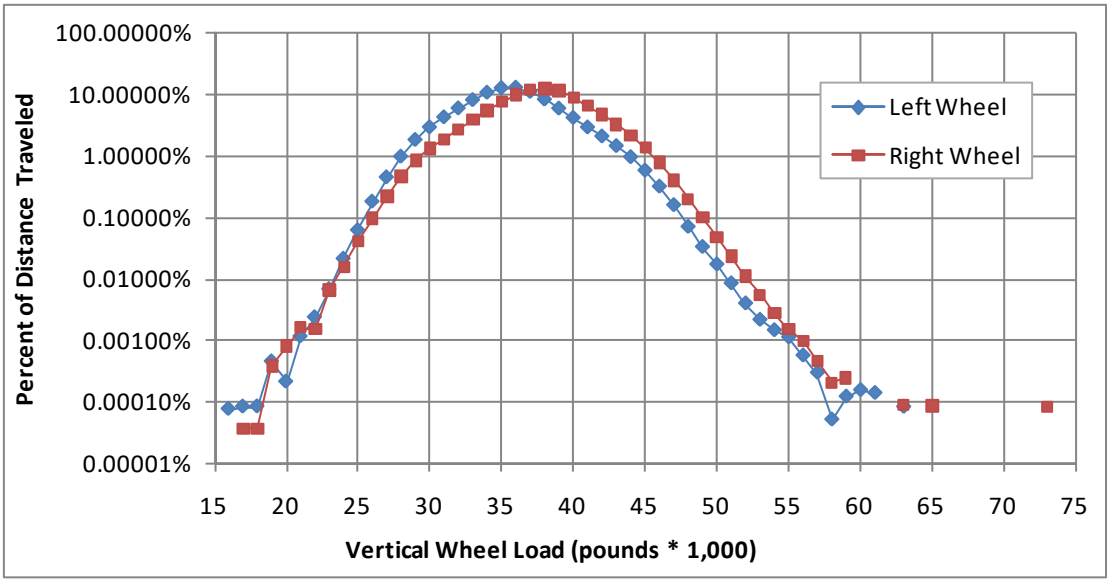

Figure 4. Histogram of Vertical Wheel/Rail Loads

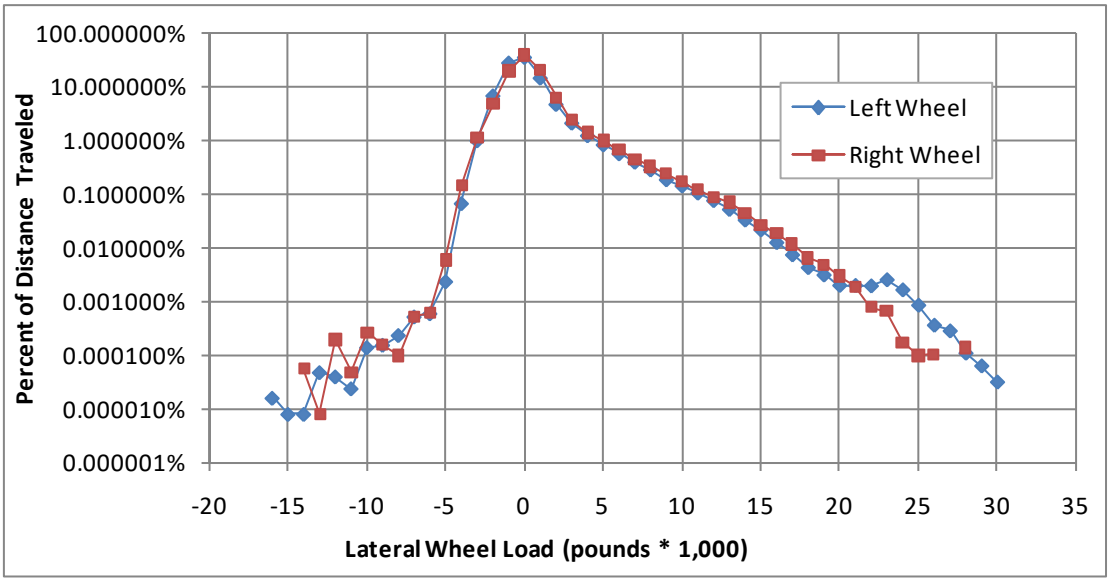

Figure 5. Histogram of Lateral Wheel/Rail Loads

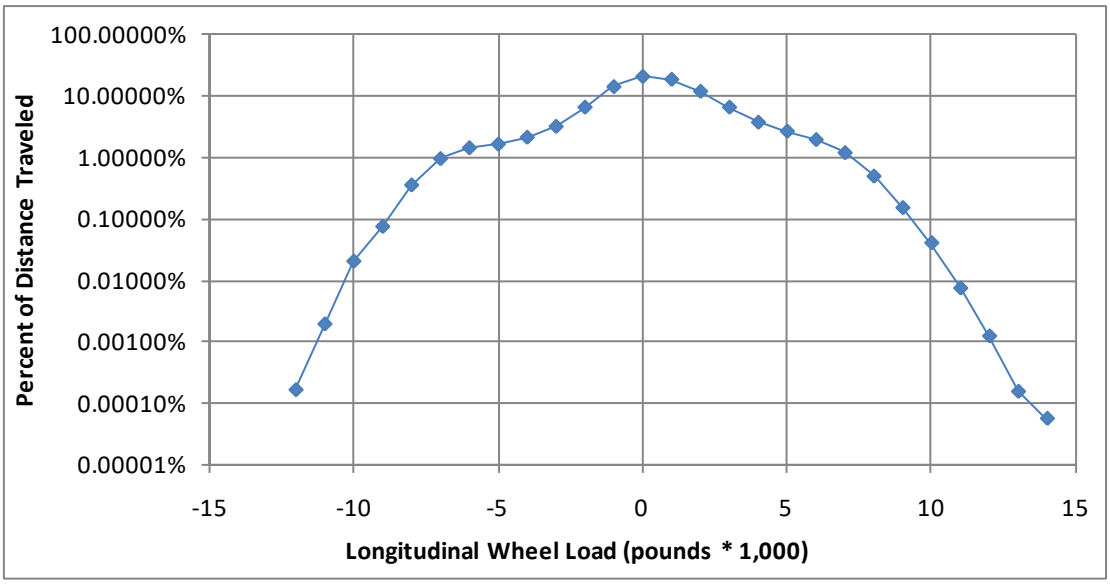

Figure 6. Histogram of Longitudinal Wheel/Rail Loads

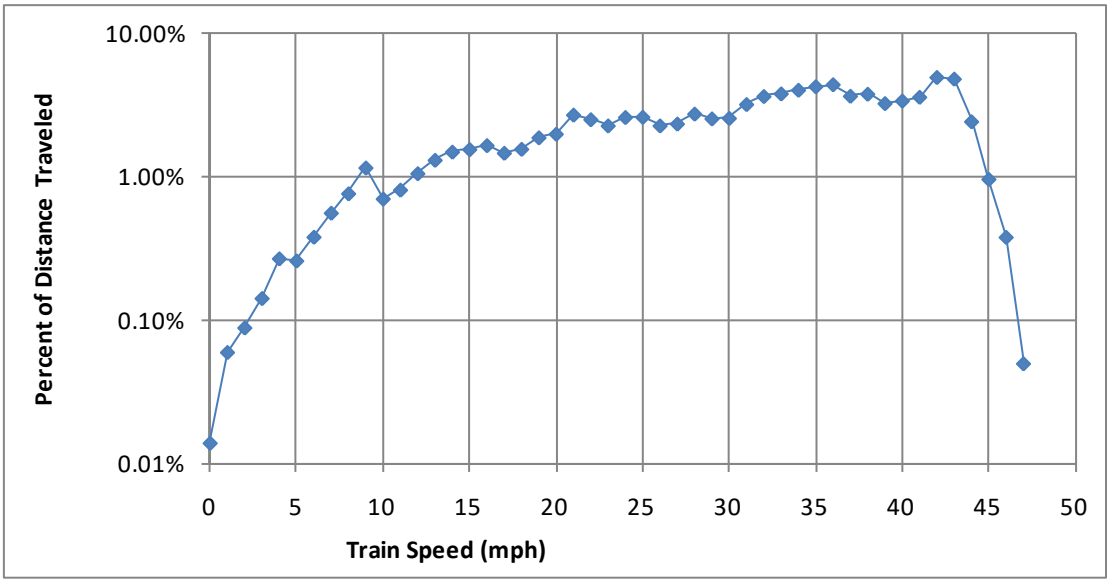

Figure 7. Histogram of Train Speed

3.1.1 Shakedown Exceedances

A total distance of 8,785 feet (1.66 miles) was traveled at conditions exceeding the shakedown limit. This represents less than 1,000 wheel circumferences (fatigue cycles) and just 0.15 percent of the loaded trip. The shakedown criteria were exceeded at the turn-around loops at the mine and power plant and at locations along the route. The longest distance traveled above the shakedown criteria at a unique track location was 704 feet. There were four unique locations with a shakedown exceedance distance of at least 575 feet and 24 unique locations with a shakedown exceedance distance of at least 100 feet. Figure 8 shows these 24 unique track locations ranked in descending order by distance traveled above the shakedown limit. The shakedown limit was exceeded at a total of 157 unique track locations.

Figure 9 shows the curvature at the top 24 unique RCF sites. Most of these sites are located in 4- to 7-degree curves. Rank ordered sites 1, 14, and 20 were inspected as discussed in Section 4, Track Inspections, of this report (later in the report, these curves are labeled D, B, and G, respectively). Rank ordered site 3 is an extremely sharp curve located in a congested urban area. Rank ordered site 18 is located on tangent track. While shakedown exceedances are occasionally expected on tangent track over short distances (less than 10 feet), due to dynamic vehicle/track interaction, this site was found to have 134 feet traveled above the shakedown limit, effectively ruling out dynamic behavior as the cause of the exceedance. Other than a nearby bridge, neither the track chart nor satellite photos show any unusual track features at this location. This site was not inspected, but potential issues with this location could include track cross-level problems or unusual rail profiles. IWS data from the second trip to verify repeatability of the problem was not available at this location.

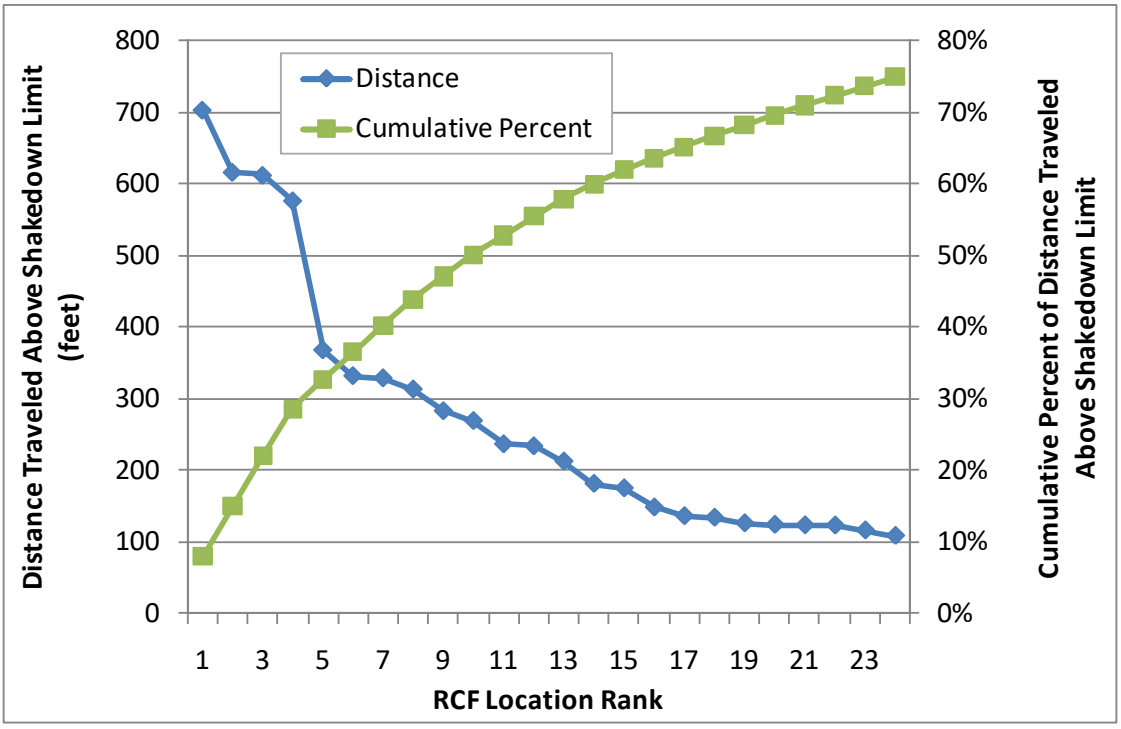

Figure 8. Distance Traveled per Shakedown Exceedance Location

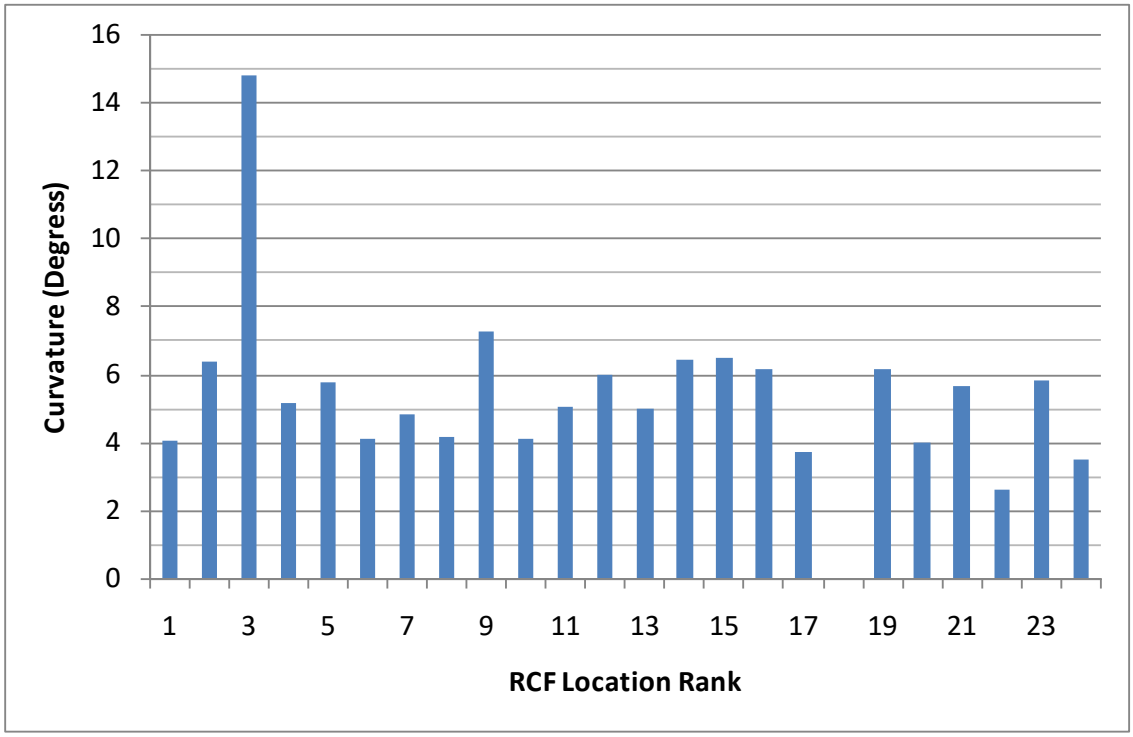

Figure 9. Curvature of Top Shakedown Exceedance Locations

Figure 10 shows the distance traveled at each curvature as well as the distance traveled at that curvature exceeding the shakedown limit. Note: a logarithmic scale is used. While the route consists mainly of tangent track and shallow curves, the majority of the distance traveled in excess of the shakedown limit occurred where the track curvature was 4 degrees or greater. In fact, 4-degree curves alone accounted for 37 percent of the total distance traveled above the shakedown limit. Figure 11 shows the percent of the total distance traveled at conditions exceeding the shakedown limit for each degree of curvature. Figure 12 shows the percent of distance traveled at each degree of curvature that exceeded the shakedown limit. Here, it can be seen that 11.7 percent of the distance traveled in 4-degree curves exceeded the shakedown limit while tighter curves all had at least 20 percent of the distance traveled above the shakedown limit. So, while there is a higher probability of exceeding the shakedown limit and accumulating RCF damage in curves tighter than 4 degrees, the much higher relative frequency of 4-degree curves makes them of prime interest in this study.

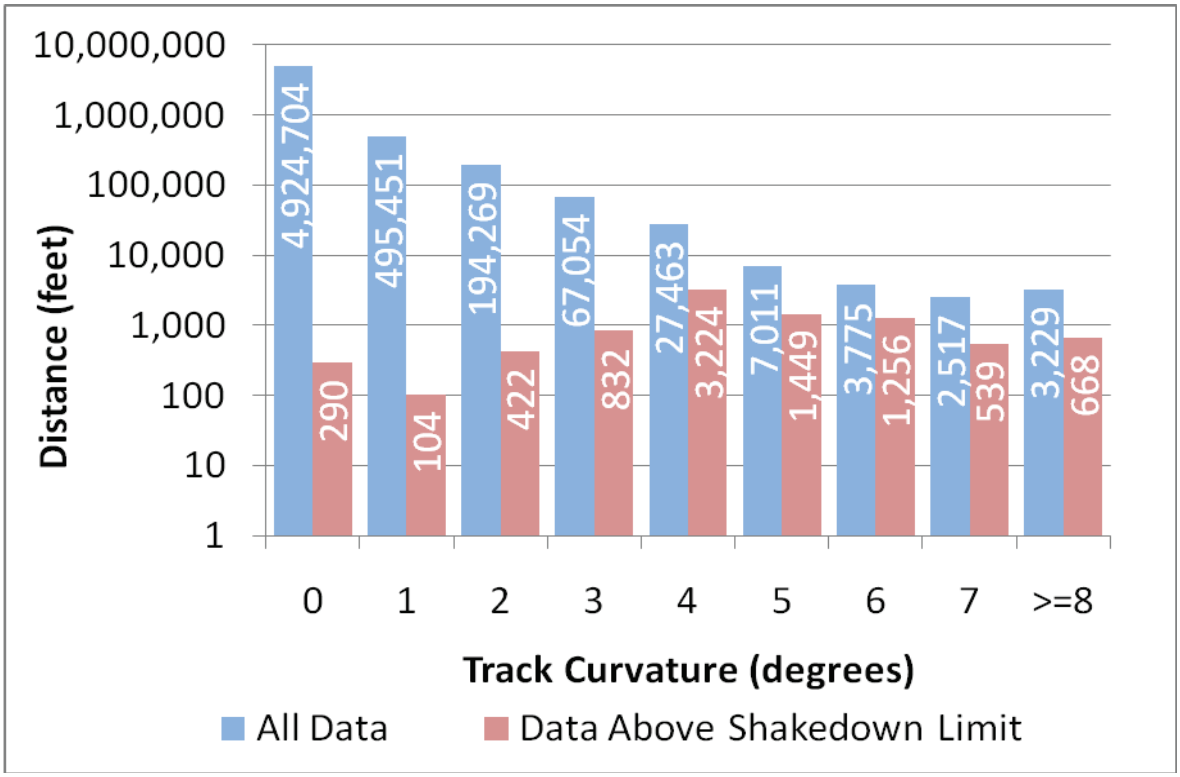

Figure 10. Distance Traveled by Track Curvature

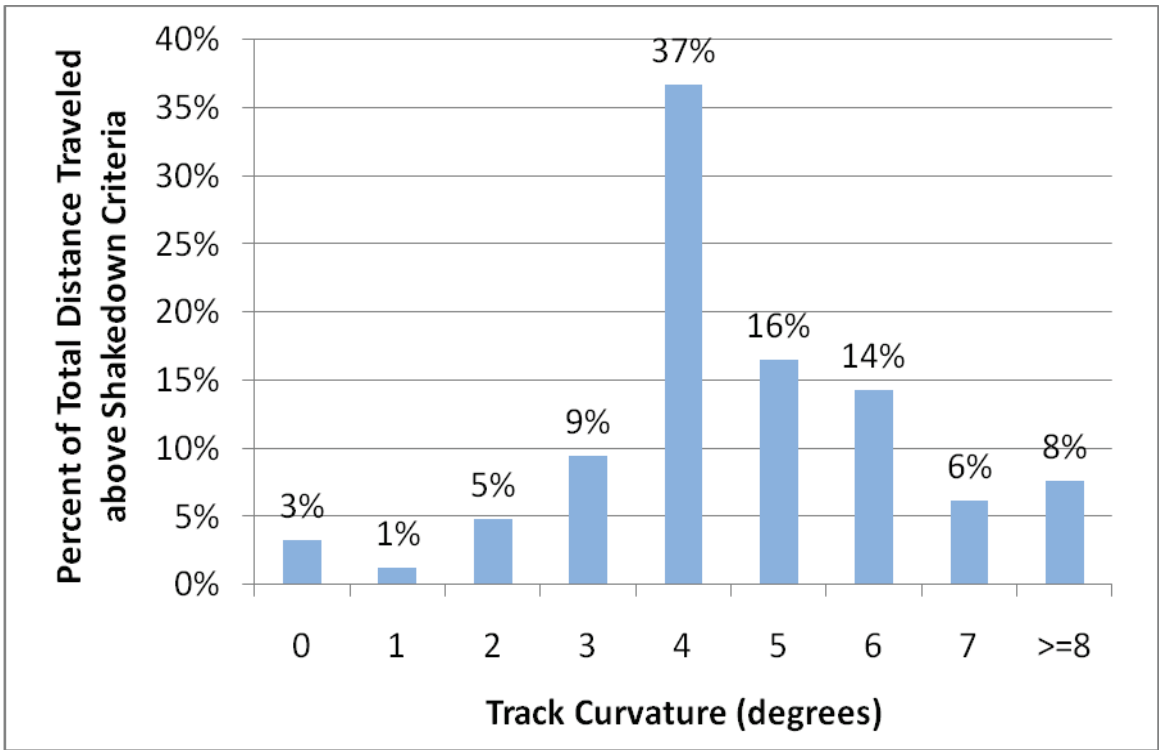

Figure 11. Relative Distribution of Track Curvature at Shakedown Exceedance Locations

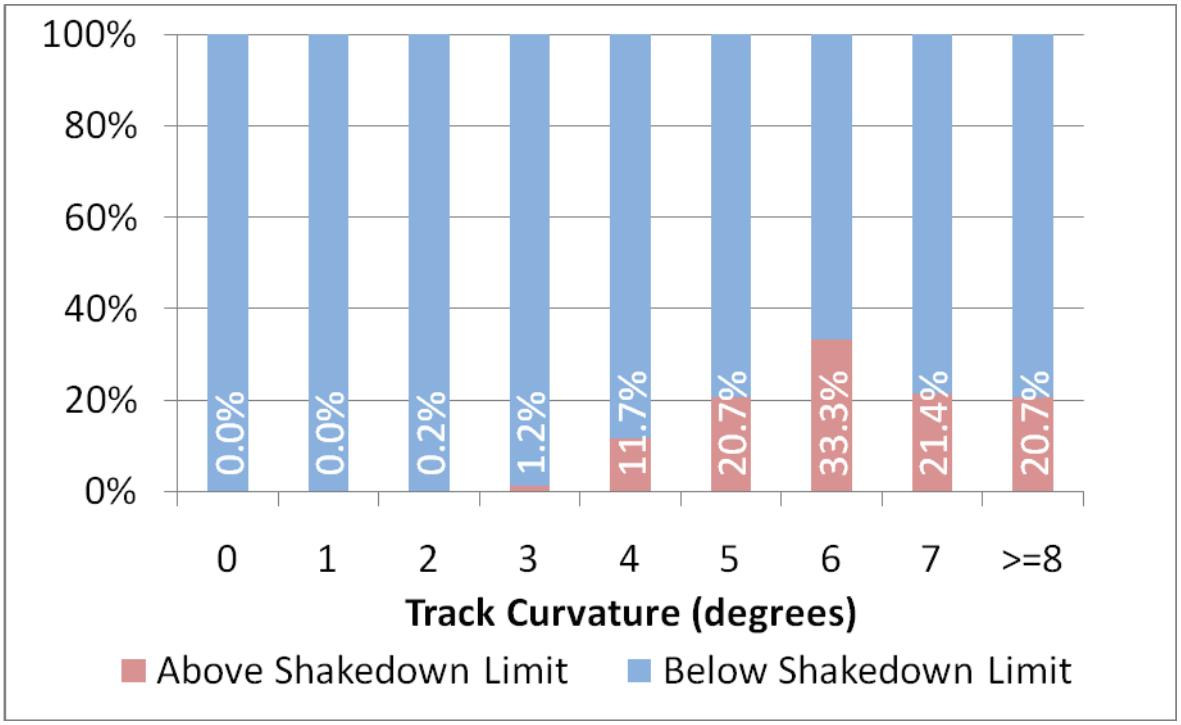

Figure 12. Percentage of Distance Traveled Above Shakedown Limit by Curvature

3.2 Second Trip

A second loaded trip over the same route began September 15, 2010, at the mine and concluded September 18, 2010, at the power plant. Due to a minor error with the system that controlled the power of the data collection computer, there were some gaps in the data recorded during the second trip. A total of 981 miles of data was recorded during the second trip. This data was used as a check of the repeatability of the readings from the first trip.

In general, wheel/rail forces had good repeatability at individual curves when comparing the first and second trips. One notable exception occurred on a 4.1-degree curve with 4 inches of superelevation. The speed limit at this site was 40 mph according to the track chart.

On the first trip, the train was traveling at 14 mph through this curve, resulting in an underbalance condition with 3.5 inches of superelevation excess. On the second trip, the train was traveling much faster at 28 mph. The train speed of the second trip resulted in a much less severe underbalance condition with 1.75 inches of superelevation excess. Figure 13 shows a contour plot of the shakedown conditions during the first trip when the shakedown limit was exceeded for a significant distance. Figure 14 shows a contour plot from the same curve during the second trip when the shakedown limit was only exceeded for a brief distance.

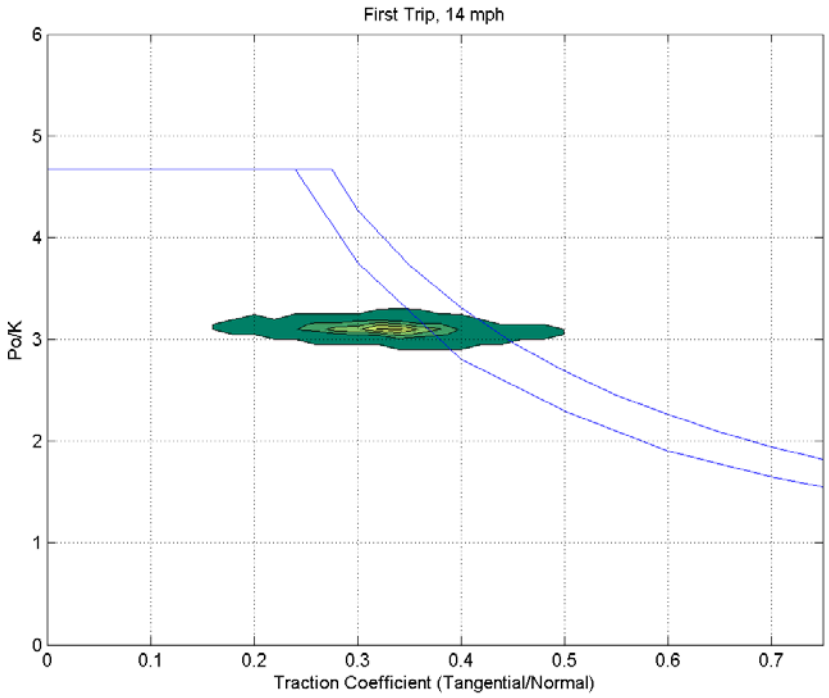

Figure 13. Shakedown Data at a 4.1-Degree Curve, First Trip, 3.5-inches Superelevation Excess

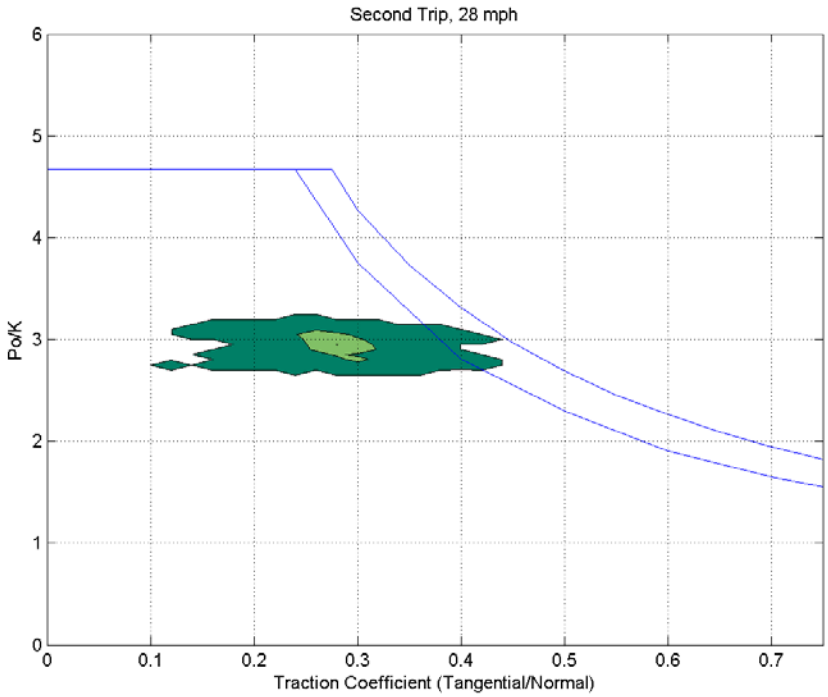

Figure 14. Shakedown Data at the Same Curve, Second Trip, 1.75-inches Superelevation Excess

The data in this curve provides an excellent example of the potential influence of train speed and track superelevation. Superelevating the outside rail in a curve is done to counteract some of the centripetal forces generated by the fastest train allowed on a particular curve. Many times, the fastest train on a curve will be a passenger train. Freight trains typically operate at lower speeds and thus do not need as much superelevation in curves to balance the smaller centripetal curving forces. Excess superelevation results in increased AOA to generate lateral wheel/rail forces necessary to offset those generated by the excess superelevation. Larger AOA values produce higher tangential wheel/rail forces, which can produce conditions exceeding the shakedown limit and accumulating RCF damage.

4. Track Inspections

Based on the wheel/rail force data, critical track sites were identified. A track inspection team was dispatched to seven sites to assess rail RCF condition and collect data on September 23, 2010. This information was compiled and analyzed to identify differences between curves where the shakedown limit was exceeded and locations of similar curvature where the shakedown limit was not exceeded.

4.1 Selection of Track Inspection Sites

Seven curves were selected for inspection based on their close proximity and similar curvature. All seven sites were located within 80 miles and on the same track subdivision. No major line branches occurred between the seven sites, ensuring that they experience nearly identical traffic. Three inspection sites had little if any exceedance of the shakedown criteria during both IWS trips. The other four sites had significant exceedance of the shakedown criteria during both IWS trips. One site had a curvature of 6.46 degrees, whereas the other sites all ranged from 4.02 to 4.25 degrees curvature.

Table 1 contains data from the track inspection sites. Each site was given an alphabetic label for ease of identification. The four inspection sites where the shakedown limit was exceeded are shown with gray background. The three inspection sites where the shakedown limit was not exceeded are shown with white background.

Table 1. Track Inspection Site Data

Site Label	Shakedown Exceeded	Relative RCF Damage Observed	High-Rail Installation Date	Low-Rail Installation Date	Lubrication Comments	Curvature Sense for Loaded Traffic	Curvature (degrees)	Average Measured Track Gage (inches)	Design Superelevation (inches)	Average Measured Superelevation (inches)	Speed Limit (mph)	Train Speed Trip 1 (mph)	Train Speed Trip 2 (mph)	Superelevation Excess Trip 1 (inches)	Superelevation Excess Trip 2 (inches)
A	No	Mild	Feb 2009	Feb 2009	Minimal residual lubricant	Left	4.20	56.5	4.0	4.3	45	24	27	2.75	2.13
B	Yes	Severe	Feb 2009	Feb 2009	Dry. Metal flakes visible.	Left	6.46	56.8	3.75	3.9	35	30	33	0.0	0.75
C	Yes	Moderate	Mar 2009	Mar 2009	Dry. Metal flakes visible.	Right	4.12	56.6	3.75	4.3	45	28	27	2.0	2.38
D	Yes	Severe	2004	2004	Dry. Metal flakes visible.	Right	4.04	56.6	3.5	3.5	45	18	20	2.5	2.38
E	No	Moderate	2004	1994	Dry. Metal flakes visible.	Left	4.12	56.8	3.75	3.5	45	28	38	1.25	-0.5
F	No	Severe	2001	2007	Dry. Metal flakes visible.	Left	4.25	56.8	5.0	5.0	45	37	N/A	1.13	N/A
G	Yes	Severe	2008	2006	Dry. Metal flakes visible.	Left	4.02	56.3	4.25	5.0	45	23	25	3.5	3.25

4.2 Results of Track Inspections

Moderate to severe RCF damage was found at each of the four curves where the IWS data exceeded the shakedown limit. The IWS data in curve A did not exceed the shakedown limit on the first trip and only briefly on the second trip. Relatively little RCF damage was found at this site. The other two of the curves (E and F) that did not cause shakedown exceedance in the IWS data showed significant RCF damage; however, consideration of the rail age and operating speeds at these curves can provide some explanation. The low rail at curve E was installed in 1994, making it at least 10 years older than any of the curves inspected. Thus, it should not be surprising that the rail has a moderate level of RCF damage after 16 years in service. curve F has a relatively large superelevation at 5 inches. Excess superelevation can cause higher axle AOA, increased tangential wheel/rail forces, and thus more RCF damage. The train carrying the vehicle with the IWS was traveling near the design speed in curve F, and the IWS data did not exceed the shakedown limit. However, trains operating at slower speeds could easily produce a situation with multiple inches of excess superelevation and would then be expected to cause RCF damage. The average train speed in this curve was not investigated in this project.

Curves A and C provide a good opportunity for a direct comparison, because the rail at both sites was installed in early 2009. The IWS data exceeded the shakedown limit at curve C, but not at curve A. Visual inspection of the rail condition showed more RCF damage at curve C compared to curve A, indicating a good correlation between the IWS data and the rail condition. The improved performance and reduced RCF at curve A could be attributable to the higher level of lubricant present. No curves had fresh lubricant present during the inspection. However, a minimal amount of lubricant was present at curve A, and it was an improvement over curve C, which was extremely dry with metal flakes on the ballast and tie plates. The residual lubricant found at curve A was on the gage face of the high rail and no lubricant was found on the low rail. While lubrication on the gage face of the high rail can reduce rail gage face wear and wheel flange wear, it is the friction on the top of the low rail that is a potential means to reduce the tangential forces that lead to RCF. With currently available wayside application systems and lubricants, lubricant applied to the rail gage face tends to migrate to the top of the rail. In areas with multiple alternating curves, the lubricant can be carried down the track from one curve to another of the opposite sense and reduce the coefficient of friction on the top of the low rail.

The track inspections occurred 19 days after the first IWS trip and 6 days after the second IWS trip. The performance at curve A was slightly worse on the second IWS trip despite a higher train speed and lower resulting superelevation excess. This may be an indication that progressively less lubricant was present, presumably on both the high and low rails, at curve A between the first IWS trip, the second IWS trip, and the track inspection. Thus, the residual lubricant found at curve A could indicate that the coefficient of friction at curve A was lower than that at curve C, particularly on the first IWS trip.

Although the rail profiles recorded at the seven track inspection sites showed differing levels of wear and material flow, all of the profiles produced highly conformal contact when matched with the wheel profiles of the IWS. Conformal contact is generally desirable and allows proper steering in curves. Some mudspots were found at curves B and G, but the track condition was otherwise considered good at these locations and all other inspection sites. Because the rail RCF was noted throughout the curves, not just near the mudspots, track condition was not considered

to be a significant factor in the RCF damage. Thus, the rail profiles at the seven inspected sites were not considered to be a significant factor in this study.

4.3 Curve Details

Photos of the rail condition at each site, rail profiles, and shakedown data are shown in the following sections for each curve site.

4.3.1 Curve A

Curve A is a 4.2-degree curve with 4.3 inches of superelevation. Figure 15 shows the condition of the low rail with relatively mild RCF cracks. Figure 16 shows the transverse profiles of the high and low rails, both installed in 2009. Minimal residual lubricant was found at this site. Figure 17 shows that the shakedown limit was not exceeded in this curve during the first trip. Figure 18 shows that minimal distance was traveled above the shakedown limit during the second trip.

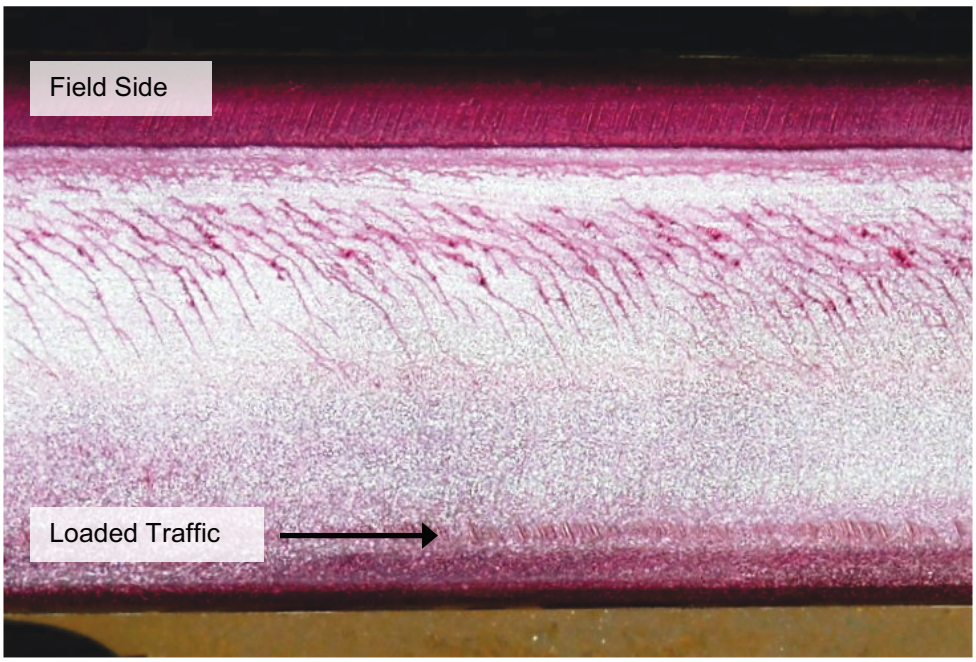

Figure 15. Photograph of Low Rail in Curve A

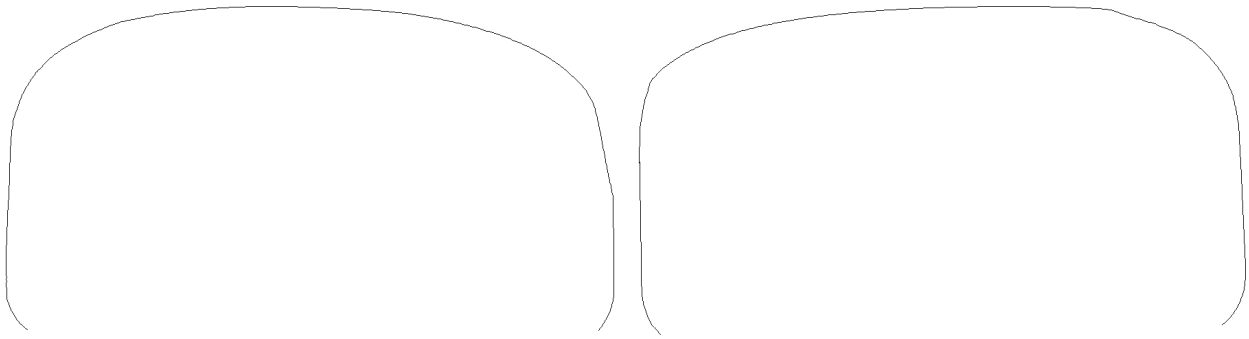

Figure 16. Curve A Rail Profiles: High Rail on the Left, Low Rail on the Right

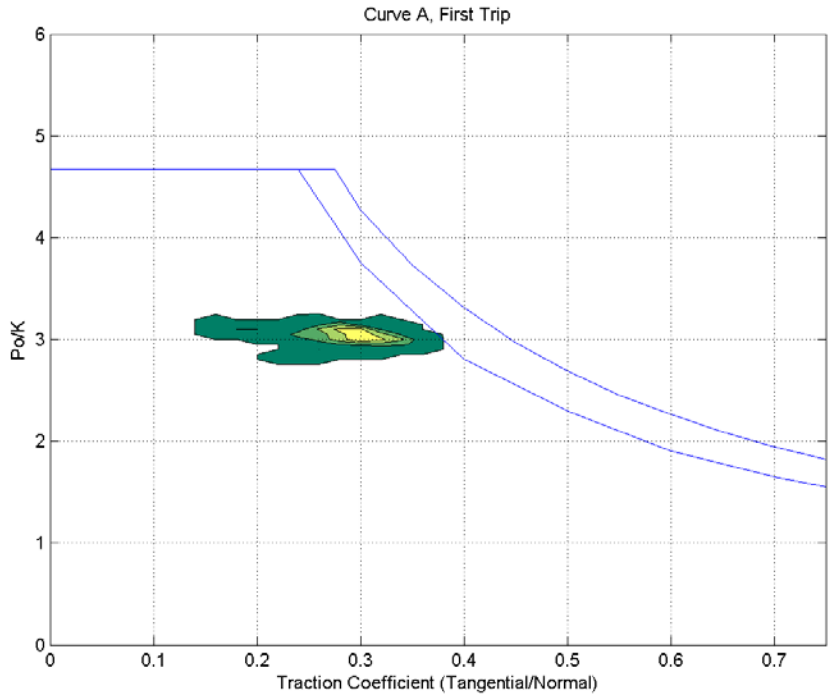

Figure 17. Curve A Shakedown Data, First Trip

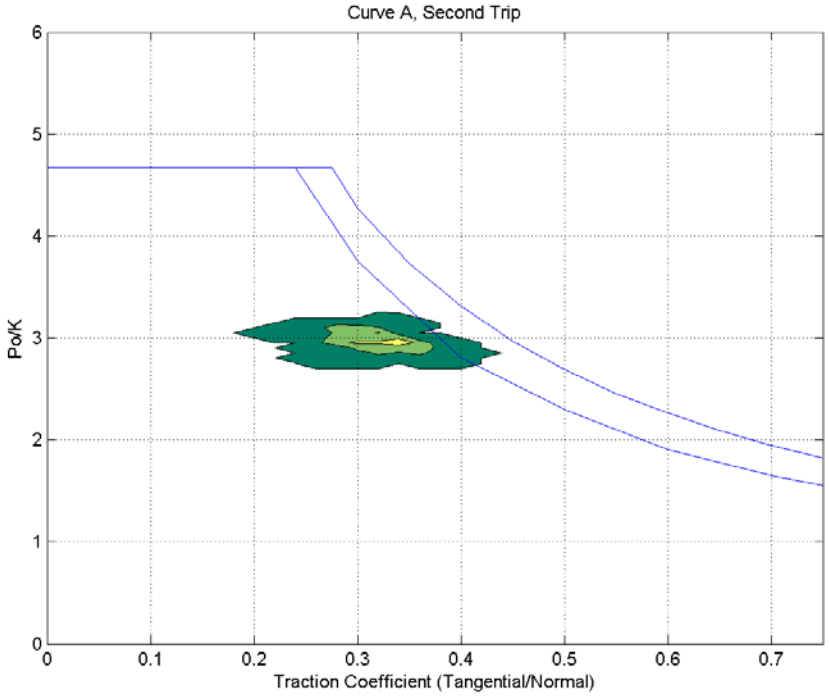

Figure 18. Curve A Shakedown Data, Second Trip

4.3.2 Curve B

Curve B is a 6.46-degree curve with 3.9 inches of superelevation. Curve B is also rank ordered site 14, as Figures 8 and 9 show. Figure 19 shows the condition of the low rail with relatively severe RCF cracks and spalls. Figure 20 shows the transverse profiles of the high and low rails, both installed in 2009. Rail at this site was extremely dry with metal wear flakes visible in the ballast. Figures 21 and 22 show that the shakedown limit was exceeded in this curve during the first and second trips, respectively.

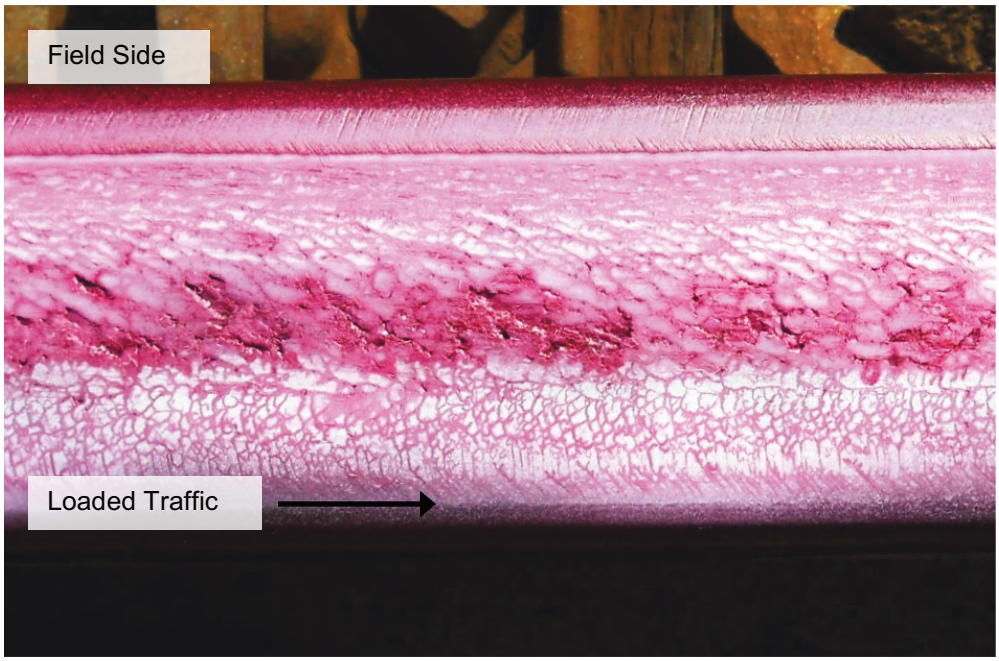

Figure 19. Photograph of Low Rail in Curve B

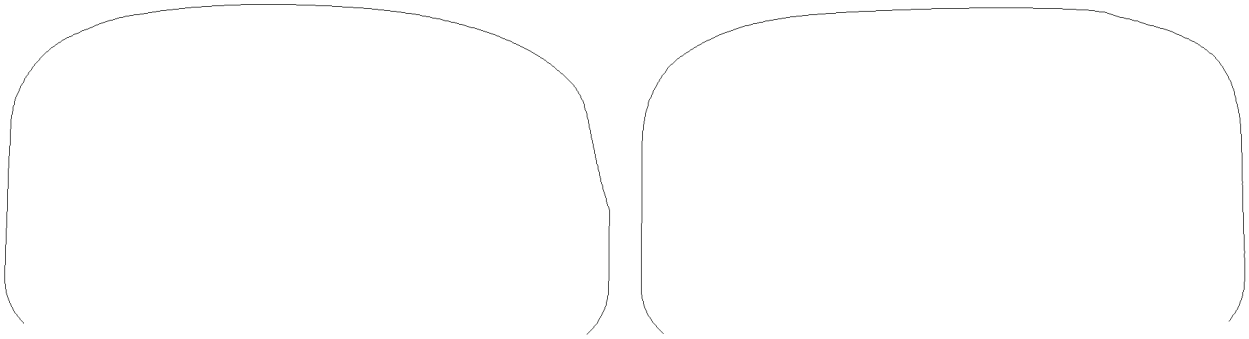

Figure 20. Curve B Rail Profiles: High Rail on the Left, Low Rail on the Right

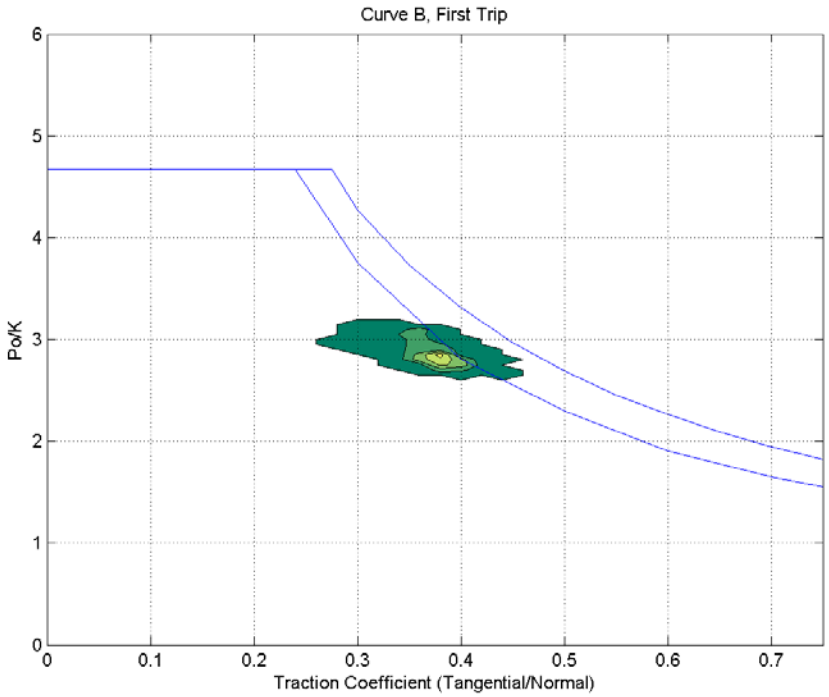

Figure 21. Curve B Shakedown Data, First Trip

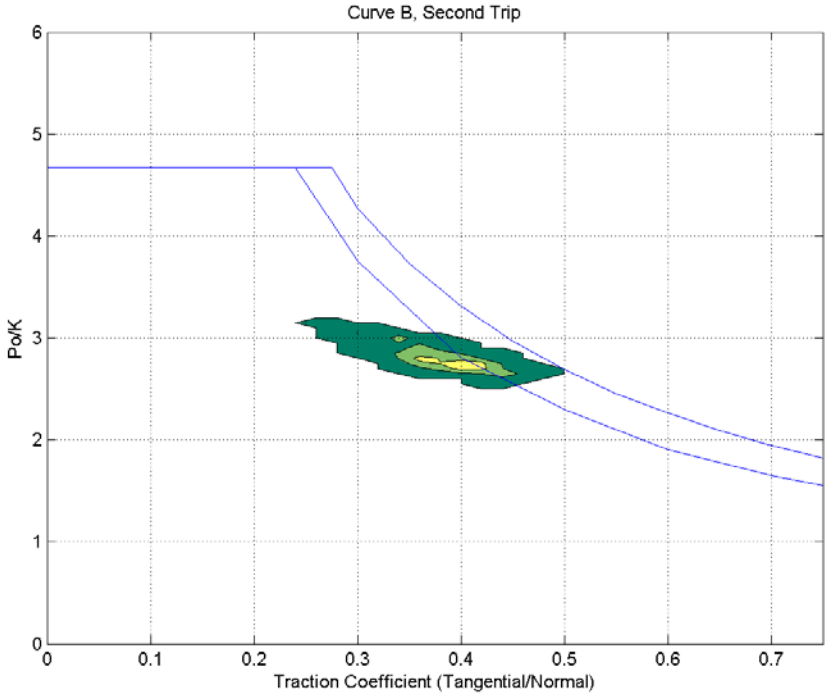

Figure 22. Curve B Shakedown Data, Second Trip

4.3.3 Curve C

Curve C is a 4.12-degree curve with 4.3 inches of superelevation. Figure 23 shows the condition of the low rail with moderate RCF cracks and tiny spalls. Figure 24 shows the transverse profiles of the high and low rails, both installed in 2009. Rail at this site was extremely dry with metal wear flakes visible in the ballast. Figures 25 and 26 show that the shakedown limit was exceeded in this curve during the first and second trips, respectively.

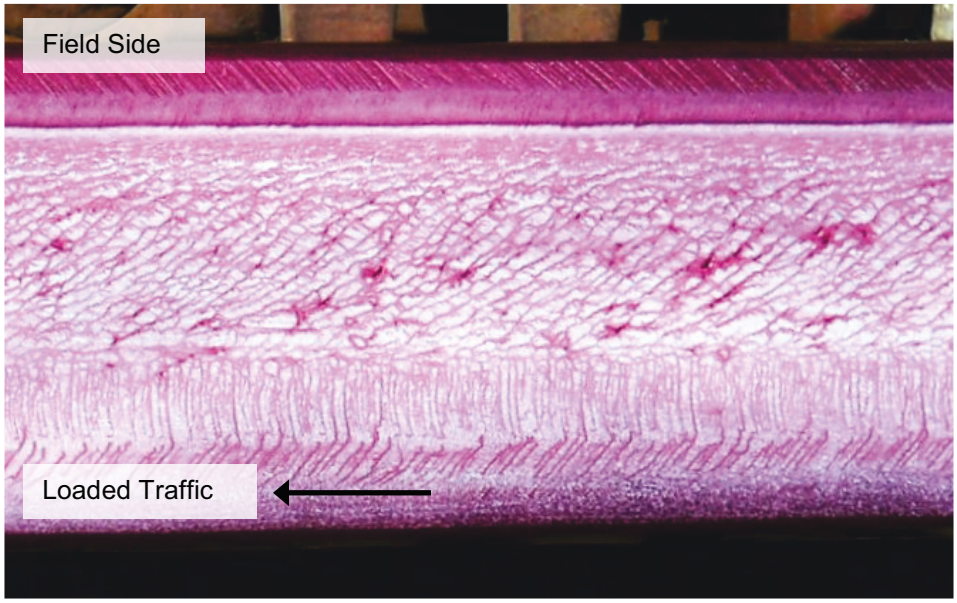

Figure 23. Photograph of Low Rail in Curve C

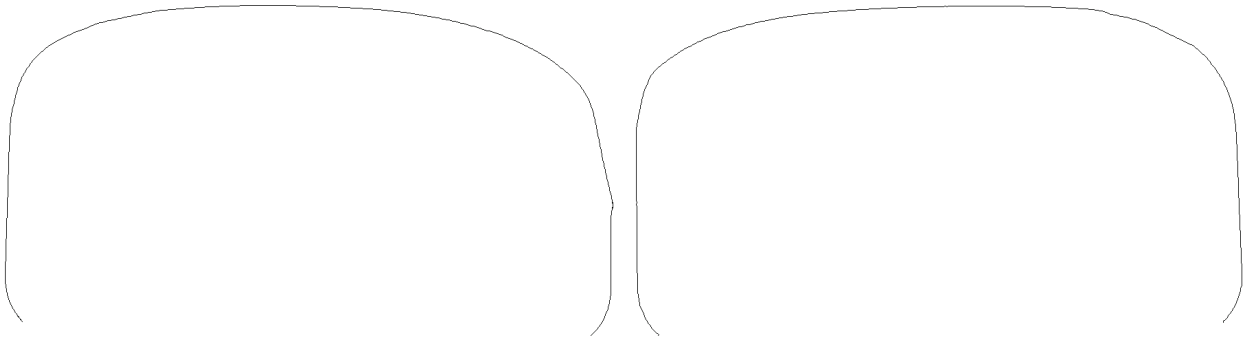

Figure 24. Curve C Rail Profiles: High Rail on the Left, Low Rail on the Right

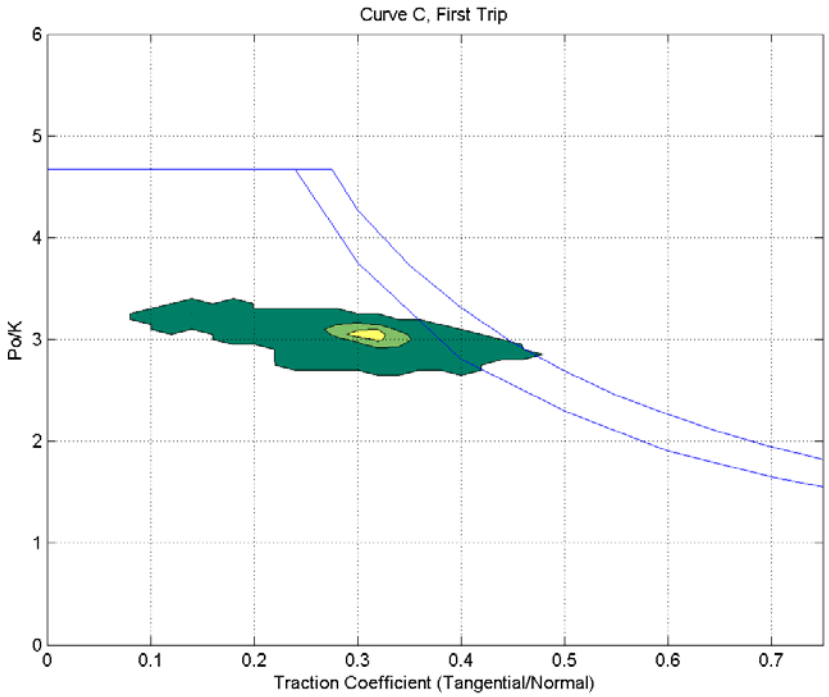

Figure 25. Curve C Shakedown Data, First Trip

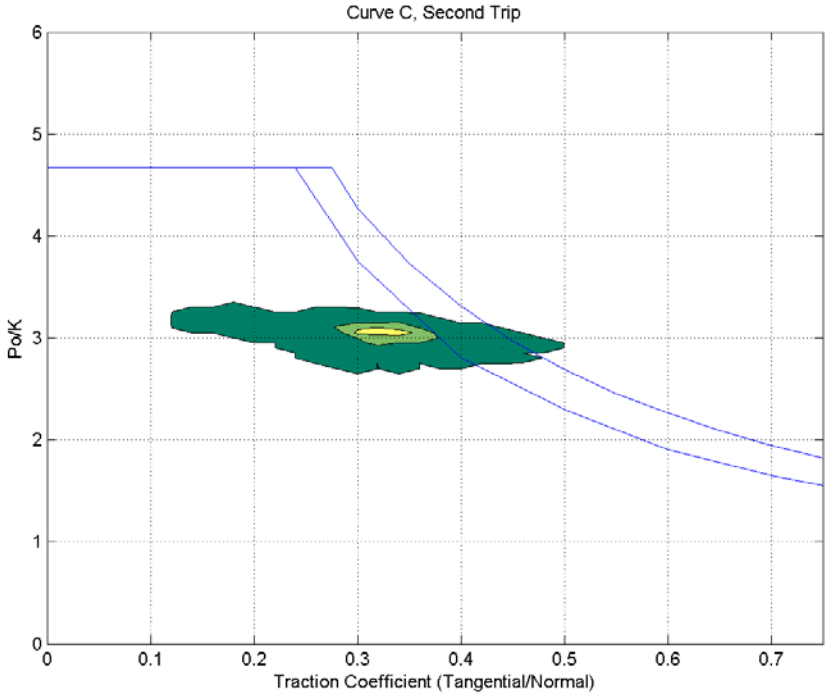

Figure 26. Curve C Shakedown Data, Second Trip

4.3.4 Curve D

Curve D is a 4.04-degree curve with 3.5 inches of superelevation. Curve D is also rank ordered site 1, as Figures 8 and 9 show. Figure 27 shows the condition of the low rail with relatively severe RCF cracks and spalls. Figure 28 shows the transverse profiles of the high and low rails, both installed in 2004. Rail at this site was extremely dry with metal wear flakes visible in the ballast. Figures 29 and 30 show that the shakedown limit was exceeded in this curve during the first and second trips, respectively.

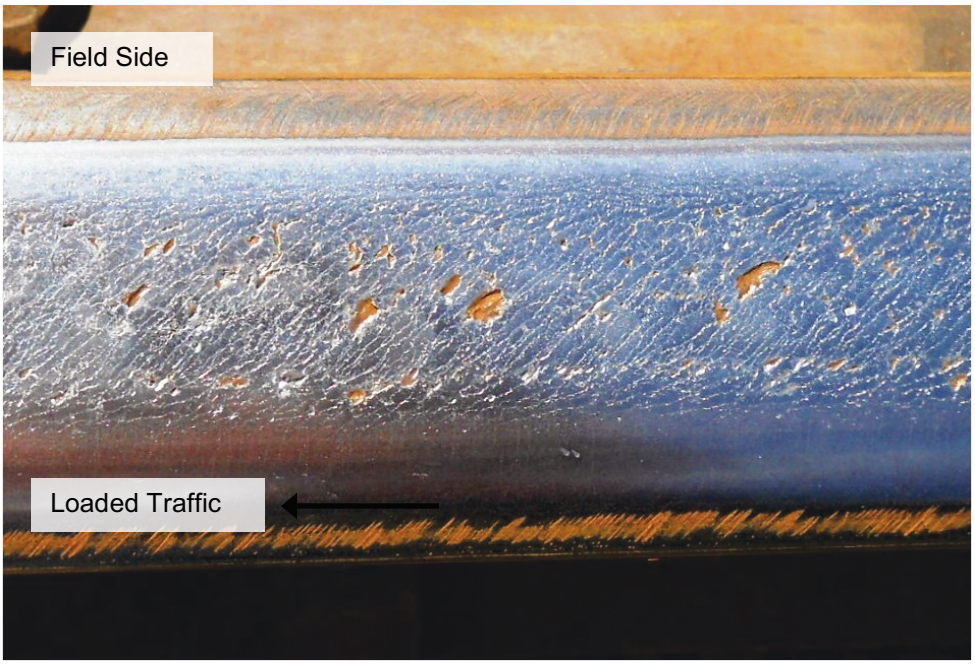

Figure 27. Photograph of Low Rail in Curve D

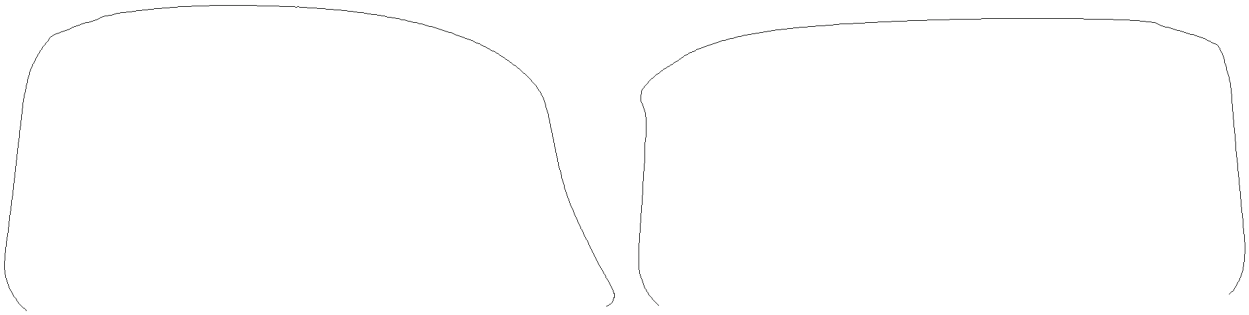

Figure 28. Curve D Rail Profiles: High Rail on the Left, Low Rail on the Right

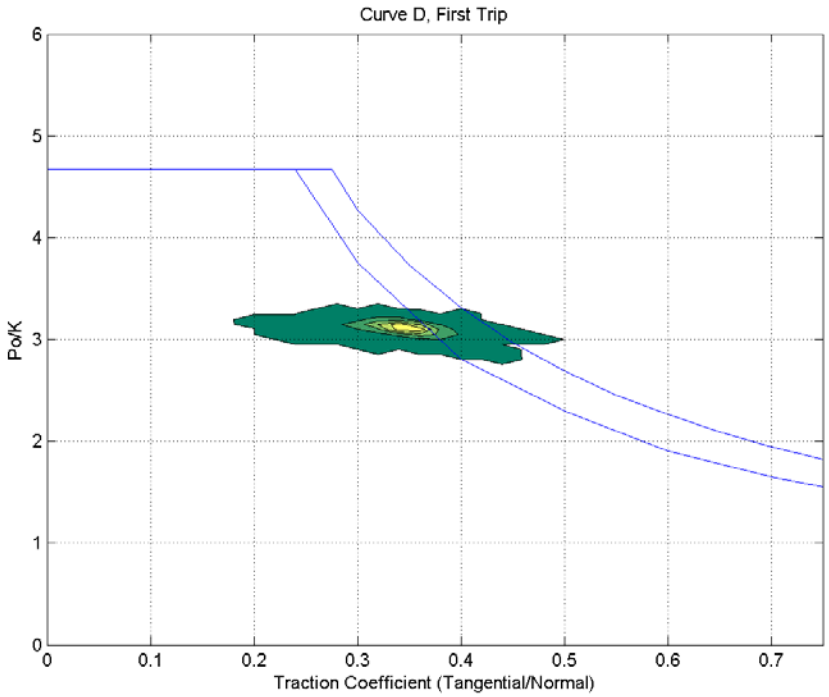

Figure 29. Curve D Shakedown Data, First Trip

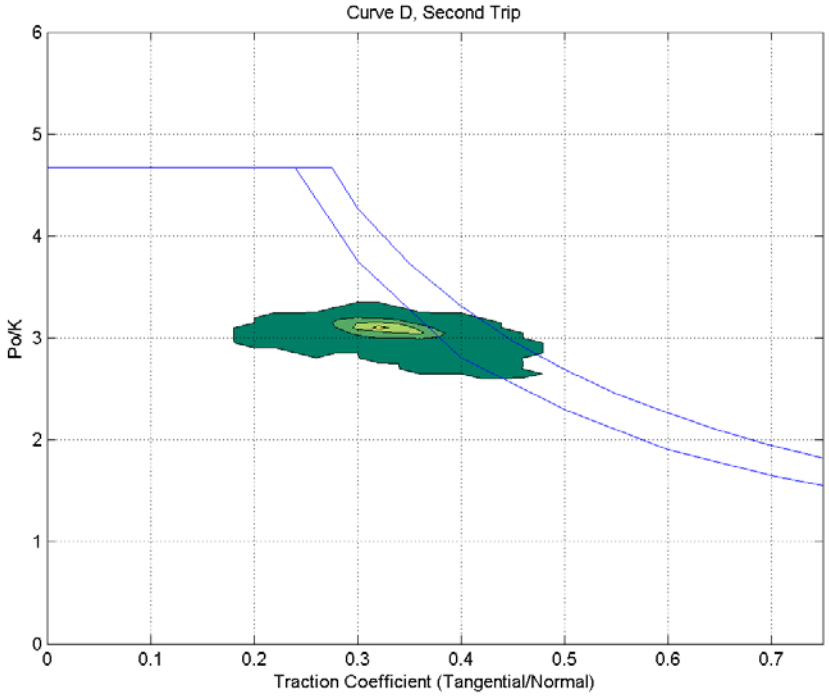

Figure 30. Curve D Shakedown Data, Second Trip

4.3.5 Curve E

Curve E is a 4.12-degree curve with 3.5 inches of superelevation. Figure 31 shows the condition of the low rail with moderate RCF cracks and small spalls. Figure 32 shows the transverse profiles of the high rail (installed in 2004) and low rail (installed in 1994). Rail at this site was extremely dry with metal wear flakes visible in the ballast. Figure 33 shows that the shakedown limit was exceeded only briefly in this curve during the first trip. Figure 34 shows that the shakedown limit was not exceeded during the second trip.

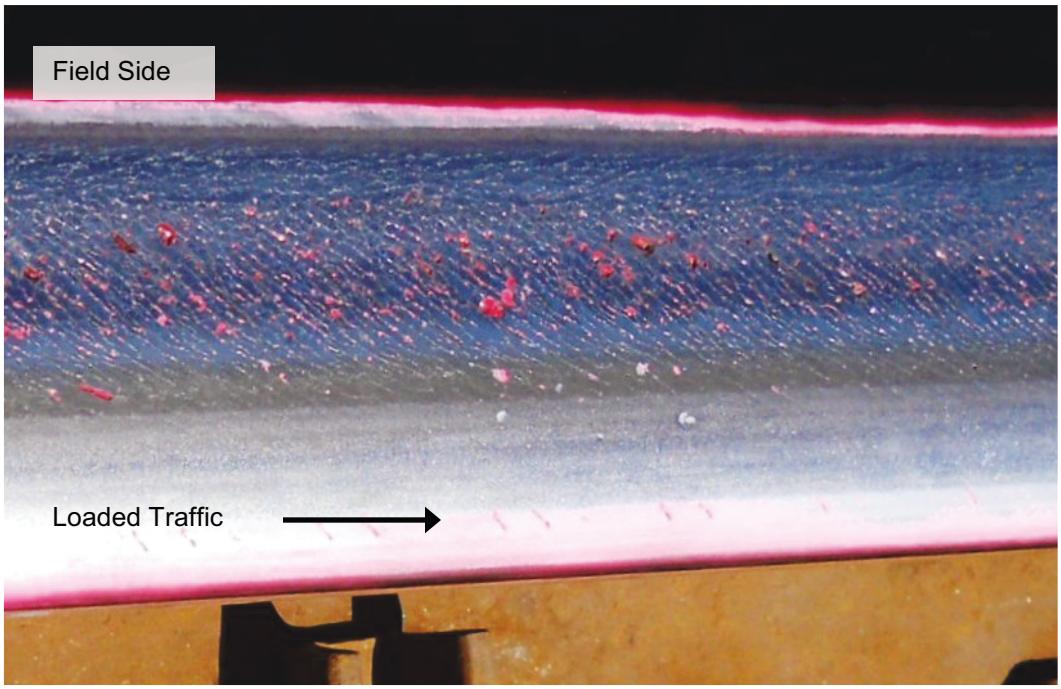

Figure 31. Photograph of Low Rail in Curve E

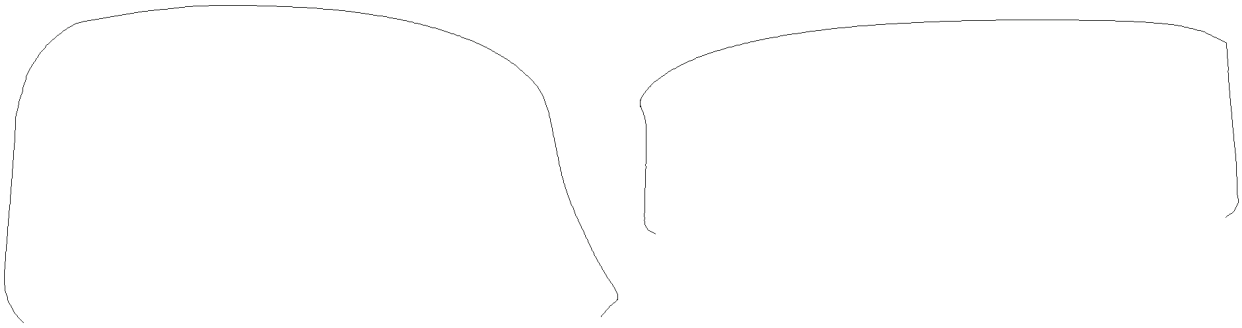

Figure 32. Curve E Rail Profiles: High Rail on the Left, Low Rail on the Right

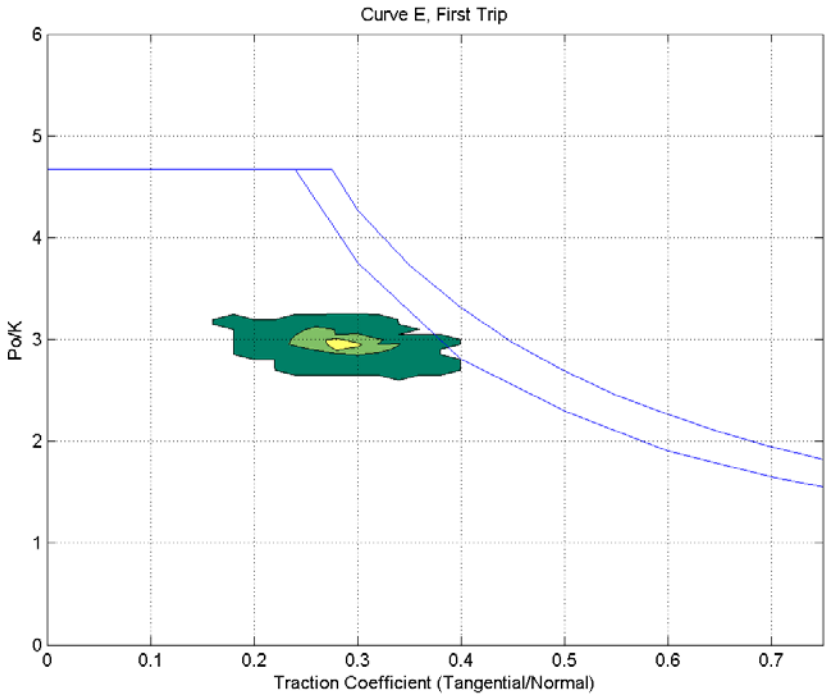

Figure 33. Curve E Shakedown Data, First Trip

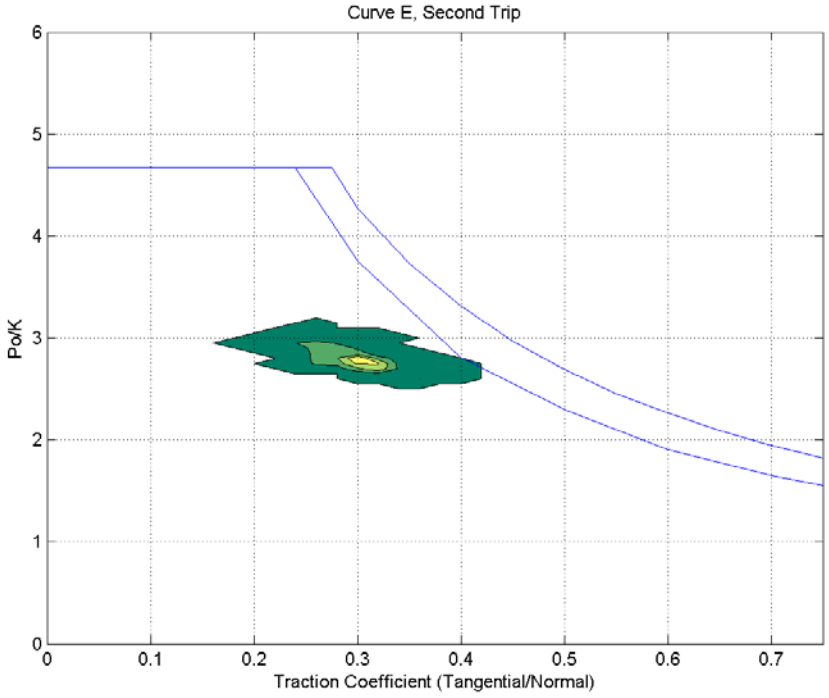

Figure 34. Curve E Shakedown Data, Second Trip

4.3.6 Curve F

Curve F is a 4.25-degree curve with 5 inches of superelevation. Figure 35 shows the condition of the low rail with relatively severe RCF cracks and small spalls. Unmatched dye penetrant and developer caused dye bleed-out, as Figure 35 shows. Figure 36 shows the transverse profiles of the high rail (installed in 2001) and low rail (installed in 2007). Rail at this site was extremely dry with metal wear flakes visible in the ballast. Figure 37 shows that the shakedown limit was not exceeded in this curve during the first trip. No data was available from this curve during the second trip.

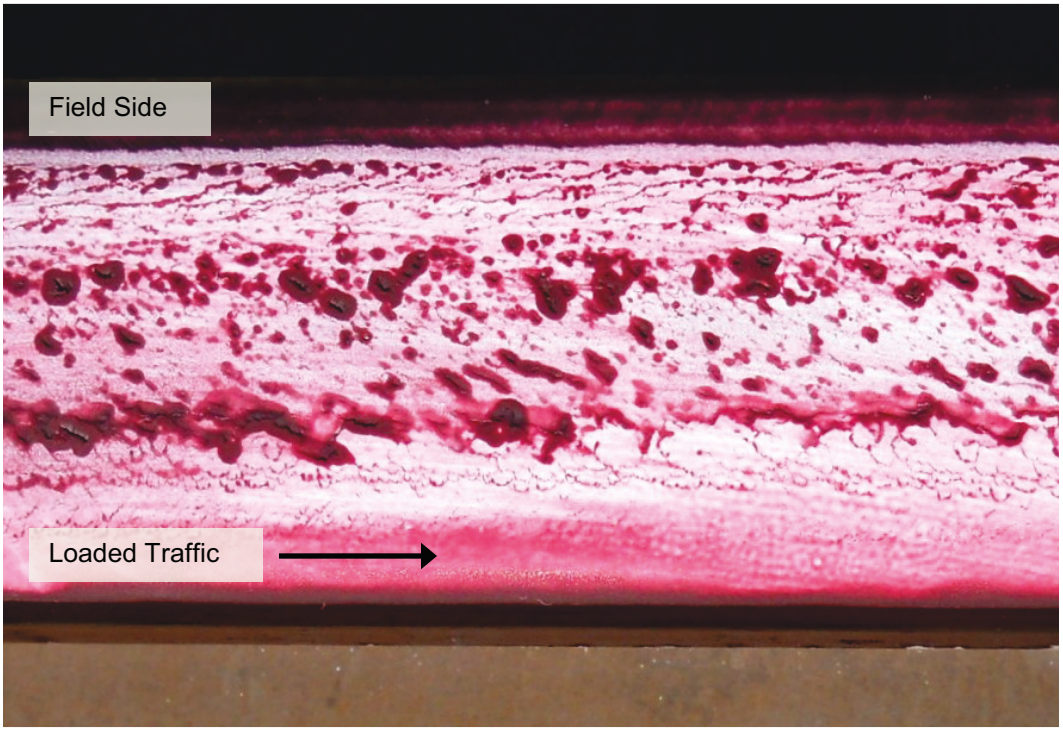

Figure 35. Photograph of Low Rail in Curve F

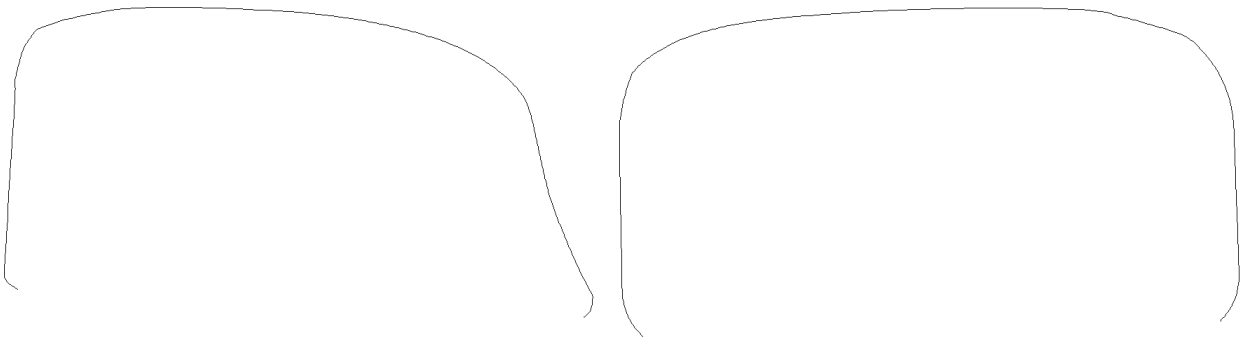

Figure 36. Curve F Rail Profiles: High Rail on the Left, Low Rail on the Right

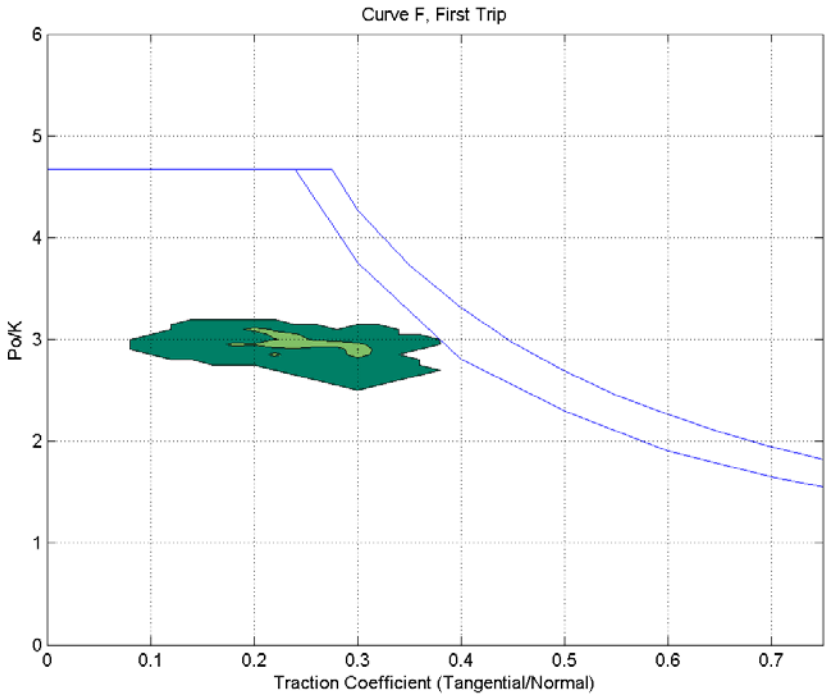

Figure 37. Curve F Shakedown Data, First Trip

4.3.7 Curve G

Curve G is a 4.02-degree curve with 5 inches of superelevation. Curve G is also rank ordered site 20, as Figures 8 and 9 show. Figure 38 shows the condition of the low rail with relatively severe RCF cracks and small spalls. Unmatched dye penetrant and developer caused dye bleed-out, as Figure 38 shows. Figure 39 shows the transverse profiles of the high rail (installed in 2008) and low rail (installed in 2006). Rail at this site was extremely dry with metal wear flakes visible in the ballast. Figures 40 and 41 show that the shakedown limit was exceeded in this curve during the first trip and second trips, respectively.

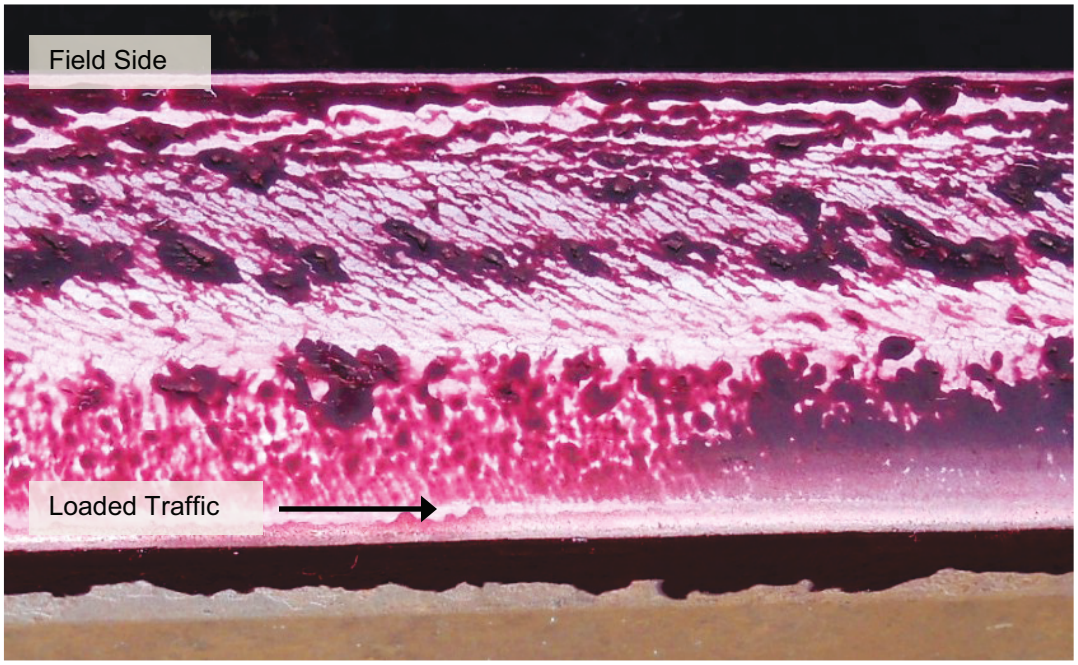

Figure 38. Photograph of Low Rail in Curve G

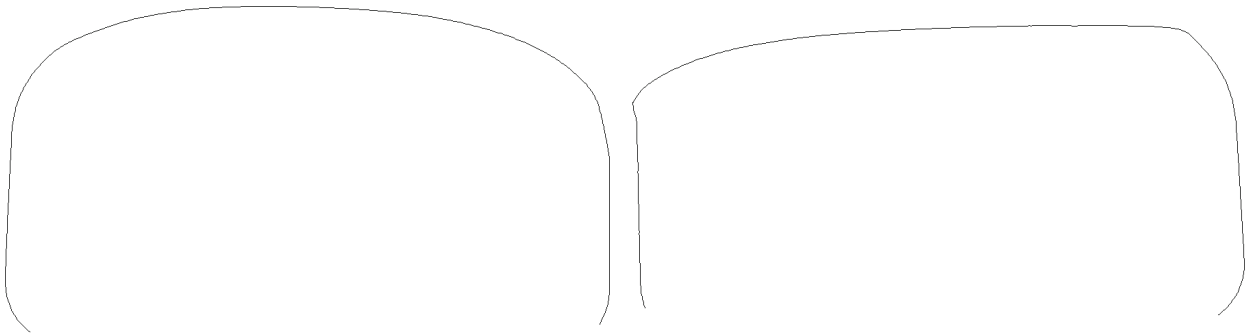

Figure 39. Curve G Rail Profiles: High Rail on the Left, Low Rail on the Right

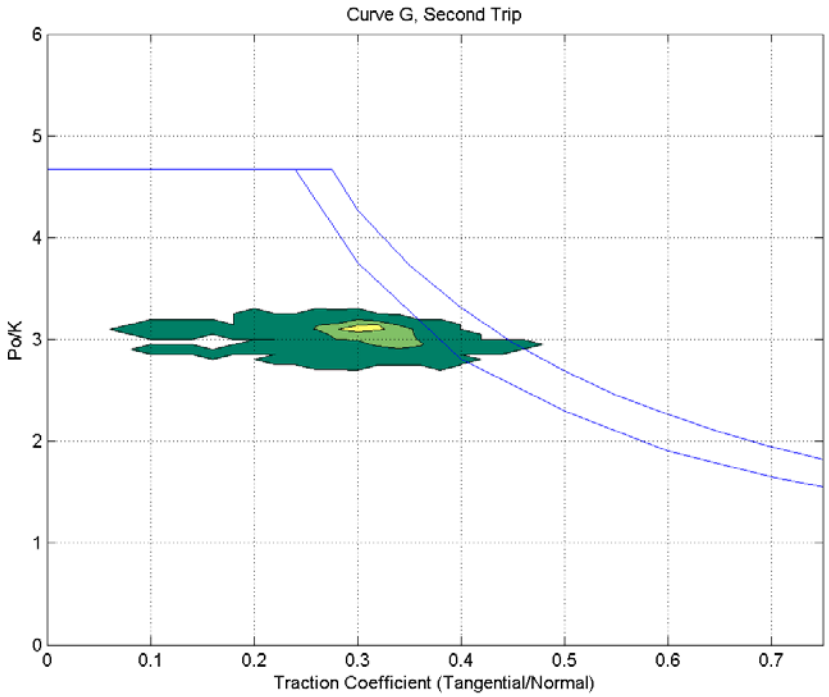

Figure 40. Curve G Shakedown Data, First Trip

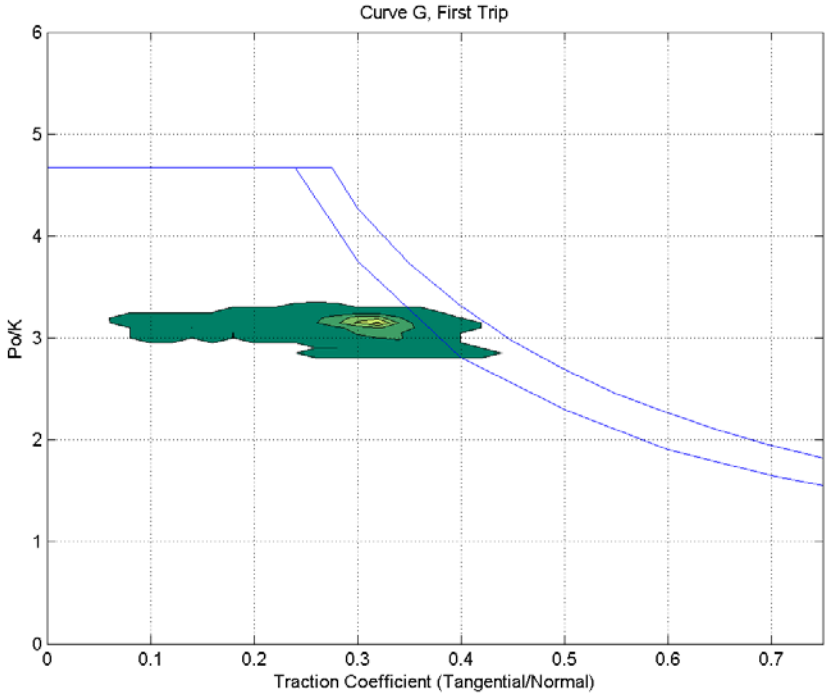

Figure 41. Curve G Shakedown Data, Second Trip

5. Conclusion

The root causes of wheel tread fatigue damage were evaluated by collecting wheel load environment data from a car running in revenue service. Track curvature, curve unbalance condition, wheel/rail coefficient of friction, were found to be factors in this study.

5.1 Findings

The findings are discussed in relation to the analysis of the wheel/rail load environment data, the track inspections, and the correlation between the two.

- Track curvature is highly influential in determining wheel and rail RCF damage. Nearly all significant shakedown exceedances were recorded on curves of at least 4 degrees.
- The combination of curvature, track superelevation, and train speed are important factors in RCF. This finding was best illustrated by the dramatic difference in performance at one curve. When operated at 14 mph and 3.5 inches of superelevation excess, the wheel/rail forces produced significant exceedance of the shakedown limit. Two weeks later, at 28 mph and 1.75 inches of superelevation excess, the shakedown limit was only briefly exceeded.
- Wheel/rail coefficient of friction in curves can be a factor in RCF. A direct comparison between two similar curves (A and C) with new rail showed that the curve with some visible residual lubricant had less RCF damage than the curve that was very dry.
- Rail profile at the locations investigated was not found to be a major factor in this analysis. The rail profiles at all inspected sites produced conformal contact with the IWS wheel profiles.
- Track condition at the locations investigated was not found to be a major factor in this analysis.
- Rail RCF condition correlated reasonably well with IWS shakedown exceedance locations.
  - Moderate to severe rail RCF damage was found at all inspected sites where the shakedown limit was exceeded (B, C, D, and G).
  - Minimal RCF damage was found at one site where shakedown was only briefly exceeded (A).
  - Moderate RCF was found at another site where shakedown was not exceeded (E) although the low rail was at least 10 years older than any other site inspected. The additional fatigue cycles accumulated at this site may be responsible for the RCF damage. The train speed was near the curve balance speed at this curve on both trips, which may help explain why the shakedown limit was not exceeded.
  - Relatively severe RCF was found at the third site where shakedown was not exceeded (F). This curve had the most superelevation of all the inspected sites. Although the train was operated at a speed to produce only a small superelevation excess while the IWS data was recorded, slower train speeds could easily produce much higher

superelevation excess values and result in large axle AOA, larger wheel/rail forces, exceedance of shakedown criteria, and accumulation of RCF damage.

5.2 Recommendations

- To reduce wheel and rail RCF, the wheel/rail coefficient of friction should be controlled in curvatures of 4 degrees or tighter. American Railway Engineering and Maintenance-of-Way Association (AREMA) guidelines for coefficient of friction are as follows [5]:
  - Gage face less than or equal to 0.20
  - Top of rail between 0.30 and 0.40
- With the understanding that passenger traffic may dictate curve superelevation, the superelevation of curves should be carefully considered in relation to typical train speed. If the typical train speed is significantly lower than the curve balance speed, it may be cost effective to reduce the superelevation in specific curves.

5.3 Future Actions

The next phase of the study involves repeating the testing with using an improved suspension.

6. References

1. Association of American Railroads. (2008). Car Repair Billing Database. Washington, D.C.
2. Duran, C. and Tournay, H. (2009). "A Parametric Analysis of Lateral Forces on a Single Wheelset Curving with an Angle of Attack," *Technology Digest* TD-09-038. Association of American Railroads, Transportation Technology Center, Inc., Pueblo, CO.
3. Cummings, S. and Lauro, D. (2008). "Inspections of Tread Damaged Wheelsets," RTDF2008-74009, *Proceedings of 2008 Fall Conference of the ASME Rail Transportation Division*, Chicago, IL.
4. Bower, A.F. and Johnson, K.L., (1991). "Plastic Flow and Shakedown of the Rail Surface in Repeated Wheel-rail Contact," *Wear*, Vol. 144, pp. 1-18.
5. American Railway Engineering and Maintenance-of-Way Association. (2009). *Manual for Railway Engineering*, Section 4.7, Recommended Practices for Rail/Wheel Friction Control, 4.7.5.3. Friction Modifiers, Lanham, MD.

Abbreviations and Acronyms

AOA	angle of attack (of an axle relative to the track)
FRA	Federal Railroad Administration
GPS	Global Positioning System
IWS	instrumented wheelset
RCF	rolling contact fatigue
TTCI	Transportation Technology Center, Inc.
UDAC	unmanned data acquisition
WILD	wheel impact load detector